

## **Newly Synthesized Imidazolium Precursors for CO<sub>2</sub> Utilization and Sequestration: Aprotic versus Protic Salts**

Abdussalam K. Qaroush,<sup>\*a</sup> Ala'a F. Eftaiha,<sup>\*b</sup> Feda'a M. Al-Qaisi,<sup>b</sup> Khaleel I. Assaf,<sup>c</sup> Suhad B. Hammad,<sup>a</sup> Malak H. Al-Anati,<sup>a</sup> Enas S. Radwan,<sup>d</sup> and Firas F. Awwadi<sup>a</sup>

<sup>a</sup> Department of Chemistry, Faculty of Science, The University of Jordan, 11942 Amman, Jordan.

<sup>b</sup> Department of Chemistry, Faculty of Science, The Hashemite University, Zarqa 13133, Jordan.

<sup>c</sup> Department of Chemistry, Faculty of Science, Al-Balqa Applied University, Al-Salt 19117, Jordan

<sup>d</sup> Faculty of Science, Zarqa University, Zarqa 13132, Jordan.

<sup>\*</sup> Corresponding Author's E-mail: [a.qaroush@ju.edu.jo](mailto:a.qaroush@ju.edu.jo); [alaa.eftaiha@hu.edu.jo](mailto:alaa.eftaiha@hu.edu.jo)

### **Electronic Supporting Information**

## Table of Contents

1	Synthesis and characterization of the catalysts.....	9
1.1	Characterization of 1,3-bis(3-(1,3-dioxoisindolin-2-yl)propyl)-1 <i>H</i> -imidazol-3-ium bromide (7).....	9
1.2	1,3-bis(3-(1,3-dioxoisindolin-2-yl)propyl)-2-methyl-1 <i>H</i> -imidazol-3-ium bromide (9) .	11
1.3	1,3-bis(3-(1,3-dioxoisindolin-2-yl)propyl)-1 <i>H</i> -benzo[ <i>d</i> ]imidazol-3-ium bromide (11).	15
1.4	1,3-dibutyl-1 <i>H</i> -imidazol-3-ium bromide (14).....	19
1.5	1,3-bis(3-ammoniopropyl)-1 <i>H</i> -imidazol-3-ium bromide (15).....	23
1.6	1,3-bis(3-aminopropyl)-1 <i>H</i> -imidazol-3-ium bromide (3).....	27
1.7	1-butyl-3-(3-(1,3-dioxoisindolin-2-yl)propyl)-1 <i>H</i> -imidazol-3-ium bromide (16).....	30
1.8	3-(3-(1,3-dioxoisindolin-2-yl)propyl)-1-hexadecyl-1 <i>H</i> -imidazol-3-ium bromide (18)..	34
1.9	6-ammoniumhexylenecarbamate (21).....	38
2	Thermal Gravimetric Analysis (TGA) .....	39
3	Cycloaddition reaction.....	40
3.1	Time Profile.....	40
3.2	<sup>1</sup> H NMR spectra of Cyclic Carbonates (CCs) reaction .....	41
3.3	<sup>1</sup> H NMR spectra for CCs Isolation.....	61
4	Proposed mechanisms of the cycloaddition reaction.....	68
5	References .....	73

<b>Figure S1.</b> $^1\text{H}$ NMR spectra of disubstituted TSIL precursor ( <b>7</b> , red trace), imidazole ( <b>5</b> , blue trace), and N-(3-bromopropyl)phthalimide ( <b>6</b> , black trace). <b>S</b> : DMSO- $d_6$ , <b>X</b> <sub>1</sub> : H <sub>2</sub> O. ....	9
<b>Figure S2.</b> $^{13}\text{C}$ NMR spectra of disubstituted TSIL precursor ( <b>7</b> , red trace), imidazole ( <b>5</b> , blue trace), and N-(3-bromopropyl)phthalimide ( <b>6</b> , black trace). <b>S</b> : DMSO- $d_6$ . ....	10
<b>Figure S3.</b> $^1\text{H}$ NMR spectrum of <b>9</b> in DMSO- $d_6$ , <b>X</b> : H <sub>2</sub> O. ....	12
<b>Figure S4.</b> $^{13}\text{C}$ NMR spectrum of <b>9</b> in DMSO- $d_6$ . ....	13
<b>Figure S5.</b> ATR-FTIR spectrum of <b>9</b> . ....	14
<b>Figure S6.</b> $^1\text{H}$ NMR spectrum of <b>11</b> in DMSO- $d_6$ , <b>X</b> <sub>1</sub> : H <sub>2</sub> O, <b>X</b> <sub>2</sub> : grease. ....	16
<b>Figure S7.</b> $^{13}\text{C}$ NMR spectrum of <b>11</b> in DMSO- $d_6$ . ....	17
<b>Figure S8.</b> ATR-FTIR spectrum of <b>11</b> . ....	18
<b>Figure S9.</b> $^1\text{H}$ NMR spectrum of <b>14</b> in DMSO- $d_6$ , <b>X</b> : H <sub>2</sub> O. ....	20
<b>Figure S10.</b> $^{13}\text{C}$ NMR spectrum of <b>14</b> in DMSO- $d_6$ . ....	21
<b>Figure S11.</b> ATR-FTIR spectrum of <b>14</b> . ....	22
<b>Figure S12.</b> $^1\text{H}$ NMR spectrum of <b>15</b> in DMSO- $d_6$ , <b>X</b> : H <sub>2</sub> O. ....	24
<b>Figure S13.</b> $^{13}\text{C}$ NMR spectrum of <b>15</b> in DMSO- $d_6$ . ....	25
<b>Figure S14.</b> ATR-FTIR spectra of 1,3-bis(3-ammoniopropyl)-1 <i>H</i> -imidazol-3-ium bromide ( <b>15</b> , red traces) and 1,3-bis(3-(1,3-dioxoisindolin-2-yl)propyl)-1 <i>H</i> -imidazol-3-ium bromide ( <b>7</b> , black traces). ....	26
<b>Figure S15.</b> $^1\text{H}$ NMR spectrum of <b>3</b> in DMSO- $d_6$ . ....	28
<b>Figure S16.</b> $^{13}\text{C}$ NMR spectrum of <b>3</b> in DMSO- $d_6$ . ....	29
<b>Figure S17.</b> $^1\text{H}$ NMR spectrum of <b>16</b> in DMSO- $d_6$ , <b>X</b> : H <sub>2</sub> O. ....	31
<b>Figure S18.</b> $^{13}\text{C}$ NMR spectrum of <b>16</b> in DMSO- $d_6$ . ....	32
<b>Figure S19.</b> ATR-FTIR spectrum of <b>16</b> . ....	33

<b>Figure S20.</b> $^1\text{H}$ NMR spectrum of <b>18</b> in $\text{CDCl}_3$ .	35
<b>Figure S21.</b> $^{13}\text{C}$ NMR spectrum of <b>18</b> in $\text{CDCl}_3$ .	36
<b>Figure S22.</b> ATR-FTIR spectrum of <b>18</b> .	37
<b>Figure S23.</b> TGA traces of imidazolium derivatives [ <b>7</b> (black trace), <b>9</b> (red trace), <b>11</b> (blue trace), <b>15</b> (green trace), <b>16</b> (purple trace), and <b>18</b> (pink trace)].	39
<b>Figure S24.</b> Reaction time profile for the conversion of ECH (1 mL) at 90 °C in DMSO (0.5 ml) using 3 mol% of <b>7</b> under atmospheric $\text{CO}_2$ pressure. Representative $^1\text{H}$ NMR spectrum for each entry is shown in Figure S26-S29.	40
<b>Figure S25.</b> $^1\text{H}$ NMR spectrum of the conversion of ECH into its corresponding carbonate in $\text{DMSO}-d_6$ , <b>S</b> : solvent, <b>X</b> : 3-chloropropane-1,2-diol (found in the original sample as supplied by the chemical vendor).	41
<b>Figure S26.</b> $^1\text{H}$ NMR spectrum of the conversion of ECH into its corresponding carbonate in $\text{DMSO}-d_6$ , <b>S</b> : solvent, <b>X</b> : 3-chloropropane-1,2-diol (from the starting material as supplied by the chemical vendor), peaks at 2.17, 3.60, 4.21, 7.72, 7.79, and 9.14 ppm correspond to the catalyst.	42
<b>Figure S27.</b> $^1\text{H}$ NMR spectrum of the conversion of ECH into its corresponding carbonate in $\text{DMSO}-d_6$ , <b>S</b> : solvent, <b>X</b> : 3-chloropropane-1,2-diol (from the starting material as supplied by the chemical vendor), peaks at 2.17, 3.60, 4.22, 7.72, 7.78, and 9.15 ppm correspond to the catalyst.	43
<b>Figure S28.</b> $^1\text{H}$ NMR spectrum of the conversion of ECH into its corresponding carbonate in $\text{DMSO}-d_6$ , <b>S</b> : solvent, <b>X</b> : 3-chloropropane-1,2-diol (from the starting material as supplied by the chemical vendor), peaks at 2.15, 3.59, 4.24, 7.71, 7.78, and 9.14 ppm correspond to the catalyst.	44
<b>Figure S29.</b> $^1\text{H}$ NMR spectrum of the conversion of ECH into its corresponding carbonate in $\text{DMSO}-d_6$ , <b>S</b> : solvent, <b>X</b> : 3-chloropropane-1,2-diol (from the starting material as supplied by the chemical vendor), peaks at 2.18, 3.62, 4.25, 7.75, 7.82, and 9.17 ppm correspond to the catalyst.	45

<b>Figure S30.</b> $^1\text{H}$ NMR spectrum of the conversion of allyl glycidyl ether into its corresponding carbonate in $\text{DMSO-}d_6$ , <b>S</b> : solvent. Peaks at 2.18, 3.62, 4.27, 7.76, 7.83, and 9.17 ppm correspond to the catalyst. ....	46
<b>Figure S31.</b> $^1\text{H}$ NMR spectrum of the conversion of 1,2-epoxy-3-phenoxy propane into its corresponding carbonate in $\text{DMSO-}d_6$ , <b>S</b> : solvent. Peaks at 2.18, 3.63, 4.23, 7.76, 7.83, and 9.18 ppm correspond to the catalyst.....	47
<b>Figure S32.</b> $^1\text{H}$ NMR spectrum of the conversion of styrene oxide into its corresponding carbonate in $\text{DMSO-}d_6$ , <b>S</b> : solvent. Peaks at 2.20, 3.65, 4.27, 7.79, 7.81, and 9.27 ppm correspond to the catalyst. ....	48
<b>Figure S33.</b> $^1\text{H}$ NMR spectrum of the conversion of cyclohexene oxide into its corresponding carbonate in $\text{DMSO-}d_6$ , <b>S</b> : solvent. Peaks at 2.16, 3.60, 4.25, 7.82, and 9.26 ppm correspond to the catalyst. ....	49
<b>Figure S34.</b> $^1\text{H}$ NMR spectrum of the conversion of 1,2-epoxybutane into its corresponding carbonate in $\text{DMSO-}d_6$ , <b>S</b> : solvent. Peaks at 2.16, 3.61, 4.24, 7.78, 7.81, and 9.19 ppm correspond to the catalyst. ....	50
<b>Figure S35.</b> $^1\text{H}$ NMR spectra in $\text{DMSO-}d_6$ of: <b>A.</b> Limonene oxide coupled with $\text{CO}_2$ in the presence of <b>7</b> , peaks at 2.17, 3.61, 4.25, 7.84 and 9.22 ppm correspond to the catalyst (blue trace); <b>B.</b> limonene oxide (orange trace). The CC peaks are not observed. Peaks at 2.18, 3.62, 4.25, 7.75, 7.82, and 9.17 ppm correspond to the catalyst. ....	51
<b>Figure S36.</b> $^1\text{H}$ NMR spectrum of the conversion of ECH into its corresponding carbonate in $\text{DMSO-}d_6$ , <b>S</b> : solvent, <b>X</b> : 3-chloropropane-1,2-diol (from the starting material purchased from the chemical vendor). Peaks at 2.09, 2.60, 3.63, 4.17, 7.64, and 7.79 ppm correspond to the catalyst. 52	

<b>Figure S37.</b> $^1\text{H}$ NMR spectrum of the conversion of ECH into its corresponding carbonate in DMSO- $d_6$ , <b>S:</b> solvent, <b>X:</b> 3-chloropropane-1,2-diol (from the starting material as supplied by the chemical vendor). Peaks at 2.31, 3.36, 3.73, 4.46, 7.79, 8.00, and 9.75 ppm correspond to the catalyst. ....	53
<b>Figure S38.</b> $^1\text{H}$ NMR spectrum of the conversion of ECH into its corresponding carbonate in DMSO- $d_6$ , <b>S:</b> solvent, <b>X:</b> 3-chloropropane-1,2-diol (from the starting material as supplied by the chemical vendor). Peaks at 2.00, 2.56, 4.29, 4.77, 7.83 and 9.14 ppm correspond to the catalyst..	54
<b>Figure S39.</b> $^1\text{H}$ NMR spectrum of the conversion of ECH into its corresponding carbonate in DMSO- $d_6$ , <b>S:</b> solvent, <b>X:</b> 3-chloropropane-1,2-diol (from the starting material as supplied by the chemical vendor). Peaks at 2.15, 2.83, 4.34, 7.71 and 9.16 ppm correspond to the catalyst.....	55
<b>Figure S40.</b> $^1\text{H}$ NMR spectrum of the conversion of ECH into its corresponding carbonate in DMSO- $d_6$ , <b>S:</b> solvent, <b>X:</b> 3-chloropropane-1,2-diol (from the starting material as supplied by the chemical vendor). Peaks at 0.87, 1.23, 1.75, 4.15, 7.70 and 9.24 ppm correspond to the catalyst..	56
<b>Figure S41.</b> $^1\text{H}$ NMR spectrum of the conversion of ECH into its corresponding carbonate in DMSO- $d_6$ , <b>S:</b> solvent, <b>X:</b> 3-chloropropane-1,2-diol (from the starting material as supplied by the chemical vendor). Peaks at 0.87, 1.24, 1.76, 2.17, 3.59, 4.15, 7.71, 7.80 and 9.20 ppm correspond to the catalyst. ....	57
<b>Figure S42.</b> $^1\text{H}$ NMR spectrum of the conversion of ECH into its corresponding carbonate in DMSO- $d_6$ , <b>S:</b> solvent, <b>X:</b> 3-chloropropane-1,2-diol (from the starting material as supplied by the chemical vendor). Peaks at 0.81, 1.18, 2.01, 3.73, 4.34, 4.46, 7.71, 7.80 and 9.14 ppm correspond to the catalyst. ....	58

<b>Figure S43.</b> $^1\text{H}$ NMR spectrum of the conversion of ECH into its corresponding carbonate in DMSO- $d_6$ , <b>S</b> : solvent, <b>X</b> : 3-chloropropane-1,2-diol (from the starting material as supplied by the chemical vendor).....	59
<b>Figure S44.</b> $^1\text{H}$ NMR spectrum of the conversion of ECH into its corresponding carbonate in DMSO- $d_6$ , <b>S</b> : solvent, <b>X</b> : 3-chloropropane-1,2-diol (from the starting material as supplied by the chemical vendor).....	60
<b>Figure S45.</b> $^1\text{H}$ NMR spectrum of the isolated 4-chloromethyl-2-oxo-1,3-dioxolane in DMSO- $d_6$ , <b>X</b> : water, traces peaks at 5.70, and 3.63 correspond to 3-chloropropane-1,2-diol. ....	62
<b>Figure S46.</b> $^1\text{H}$ NMR spectrum of the isolated 4-((allyloxy)methyl)-1,3-dioxolan-2-one in DMSO- $d_6$ , <b>X</b> : water. ....	63
<b>Figure S47.</b> $^1\text{H}$ NMR spectrum of the isolated 4-phenyl-1,3-dioxolan-2-one in DMSO- $d_6$ , <b>X</b> : water. ....	64
<b>Figure S48.</b> $^1\text{H}$ NMR spectrum of 4-(phenoxymethyl)-1,3-dioxolan-2-one in DMSO- $d_6$ .....	65
<b>Figure S49.</b> $^1\text{H}$ NMR spectrum of 4-ethyl-1,3-dioxolan-2-one in DMSO- $d_6$ . ....	66
<b>Figure S50.</b> $^1\text{H}$ NMR spectrum of 4-phenyl-1,3-dioxolan-2-one in DMSO- $d_6$ isolated from the recyclability run, <b>X</b> : water. ....	67
<b>Figure S51.</b> DFT-optimized molecular geometries of the species present in the reaction profile of ECH and $\text{CO}_2$ , see Figure 9A. ....	70
<b>Figure S52.</b> Packing diagram of <b>15</b> viewed down the a-axis.....	71
 <b>Scheme S1.</b> Synthetic route of 1,3-bis(3-(1,3-dioxoisindolin-2-yl)propyl)-2-methyl-1 <i>H</i> -imidazol-3-ium bromide ( <b>9</b> ). ....	11

<b>Scheme S2.</b> Synthetic route of 1,3-bis(3-(1,3-dioxoisindolin-2-yl)propyl)-1 <i>H</i> -benzo[ <i>d</i> ]imidazol-3-ium bromide ( <b>11</b> ). .....	15
<b>Scheme S3.</b> Synthetic route of 1,3-dibutyl-1 <i>H</i> -imidazol-3-ium bromide ( <b>14</b> ). .....	19
<b>Scheme S4.</b> Synthetic route of 1,3-bis(3-ammoniopropyl)-1 <i>H</i> -imidazol-3-ium bromide ( <b>15</b> ).....	23
<b>Scheme S5.</b> Synthetic route of 1,3-bis(3-aminopropyl)-1 <i>H</i> -imidazol-3-ium bromide ( <b>3</b> ).....	27
<b>Scheme S6.</b> Synthetic route of 1-butyl-3-(3-(1,3-dioxoisindolin-2-yl)propyl)-1 <i>H</i> -imidazol-3-ium bromide ( <b>16</b> ).....	30
<b>Scheme S7.</b> Synthetic route of 3-(3-(1,3-dioxoisindolin-2-yl)propyl)-1-hexadecyl-1 <i>H</i> -imidazol-3-ium bromide ( <b>18</b> ). .....	34
<b>Scheme S8.</b> Synthetic route for the production of <b>21</b> .....	38
<b>Scheme S9.</b> Proposed reaction mechanism of ECH conversion into its corresponding carbonate using catalyst <b>7</b> .....	68
<b>Scheme S10.</b> Proposed reaction mechanism of ECH conversion into its corresponding carbonate using catalyst <b>9</b> .....	69



# 1 Synthesis and characterization of the catalysts

## 1.1 Characterization of 1,3-bis(3-(1,3-dioxisoindolin-2-yl)propyl)-1*H*-imidazol-3-ium bromide (7)

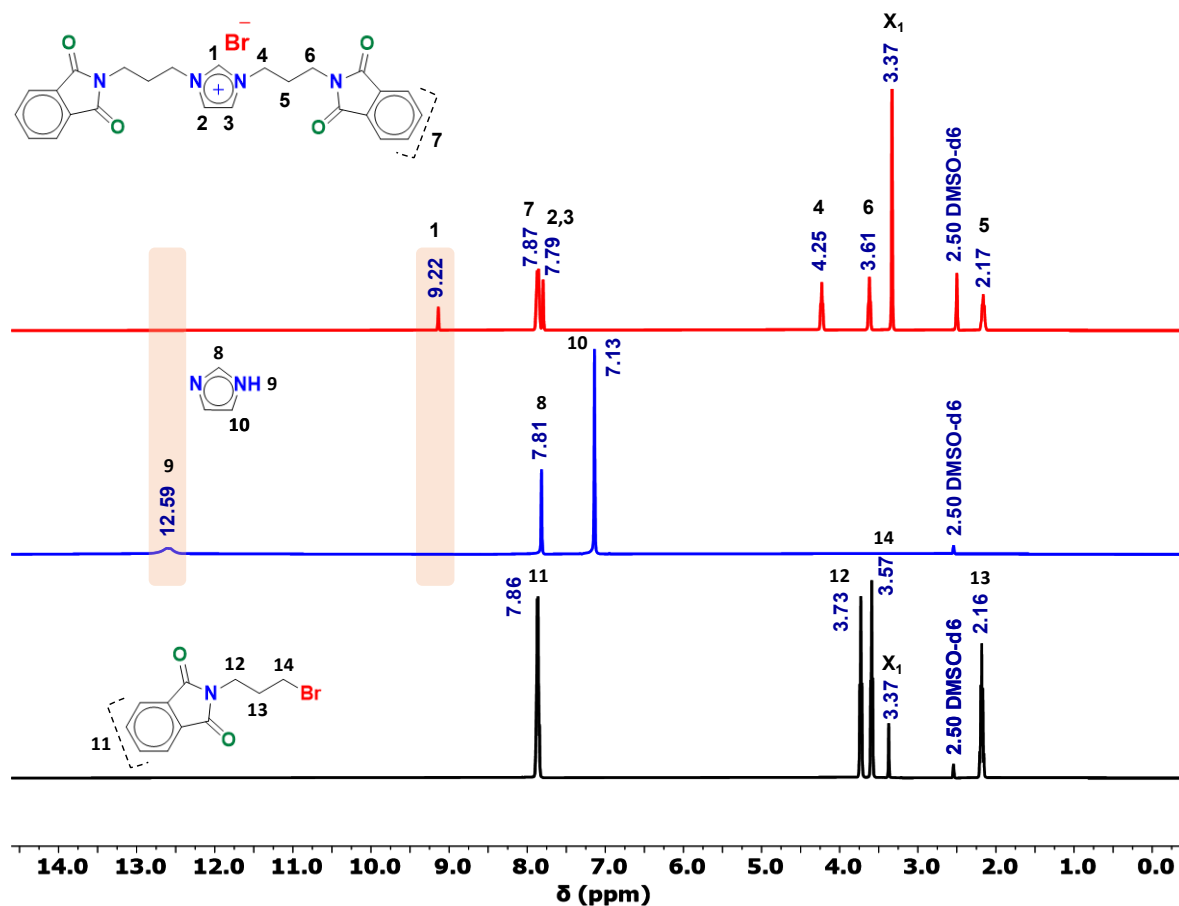


**Figure S1.** <sup>1</sup>H NMR spectra of disubstituted TSIL precursor (7, red trace), imidazole (5, blue trace), and N-(3-bromopropyl)phthalimide (6, black trace). S: DMSO-*d*<sub>6</sub>, X<sub>1</sub>: H<sub>2</sub>O.

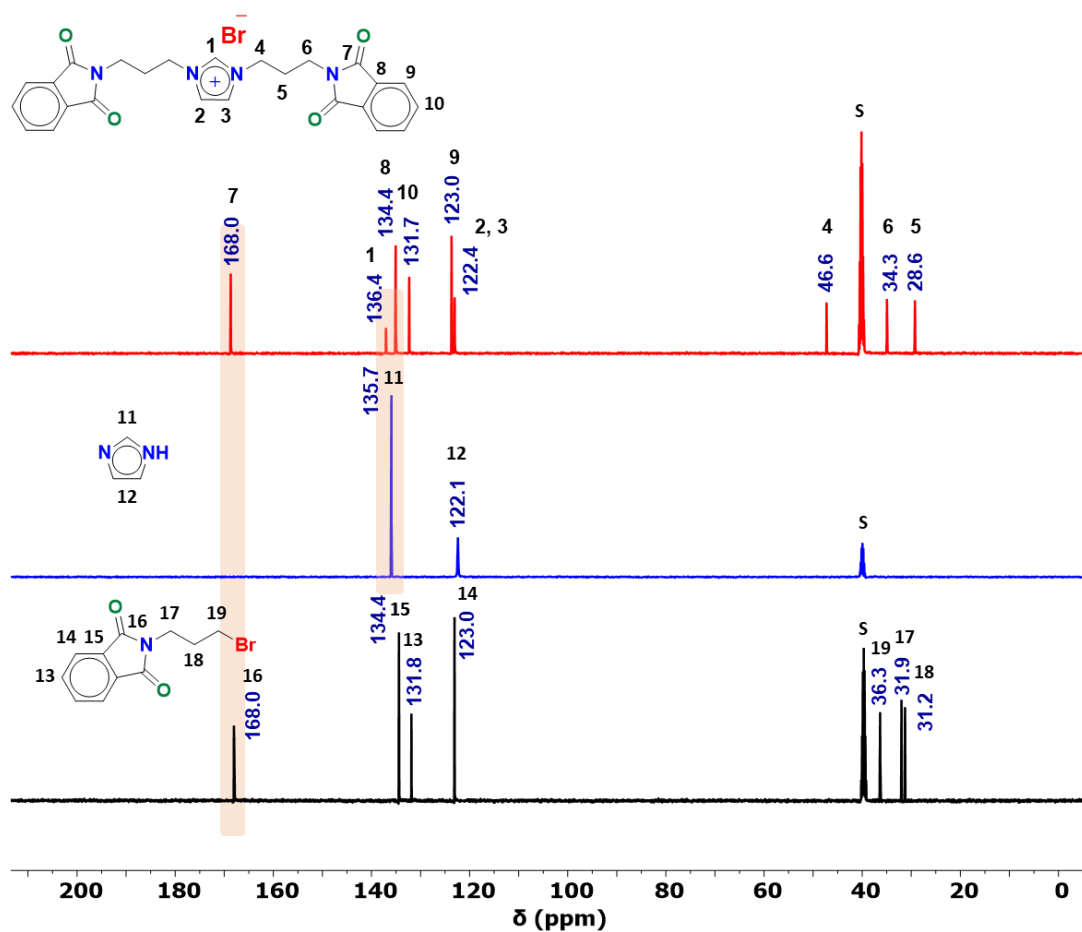
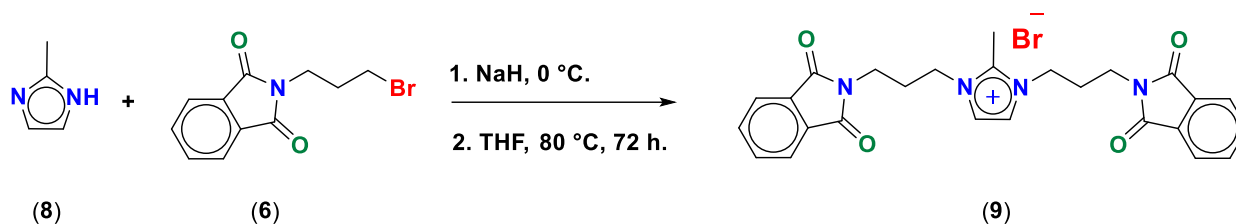


**Figure S2.**  $^{13}\text{C}$  NMR spectra of disubstituted TSIL precursor (7, red trace), imidazole (5, blue trace), and N-(3-bromopropyl)phthalimide (6, black trace). S:  $\text{DMSO-}d_6$ .

## 1.2 1,3-bis(3-(1,3-dioxoisindolin-2-yl)propyl)-2-methyl-1*H*-imidazol-3-ium bromide (9)



**Scheme S1.** Synthetic route of 1,3-bis(3-(1,3-dioxoisindolin-2-yl)propyl)-2-methyl-1*H*-imidazol-3-ium bromide (9).

In a three-neck, 250 mL, round-bottomed flask equipped with a magnetic stirring bar, condenser, dropping funnel, and a glass stopper. A solution of 2-methyl imidazole (8, 0.839 g, 10.23 mmol) in 20 mL of anhydrous THF was added dropwise over a period of 2 h with continuous stirring at 0 °C to a suspended solution of NaH (0.45 g, 11.25 mmol, 30 ml THF). The mixture left with continuous stirring at 0 °C for another 2 h. Then, a solution of N-(3-bromopropyl) phthalimide (6, 6.16 g, 22.97 mmol, 2.2 *eq.*) in another 30 mL THF was dropwise-added to the reaction mixture over a period of 2 h. Once completed, it was stirred at room temperature (RT) for another 2 h. After that, the reaction mixture was refluxed for a period of 72 h at 80 °C under continuous stirring. The white precipitate was washed with 100 mL as-received THF, then dissolved in acetonitrile to get rid of remaining solid of NaBr. After the filtration, the filtrate was evaporated, and the isolated product was dried under vacuum with yield up to 67. **HRMS** ( $m/z$  of  $[C_{26}H_{25}N_4O_4]^+$ , Calculated: 457.18703. Found: 457.19235). Melting point = 262 °C.

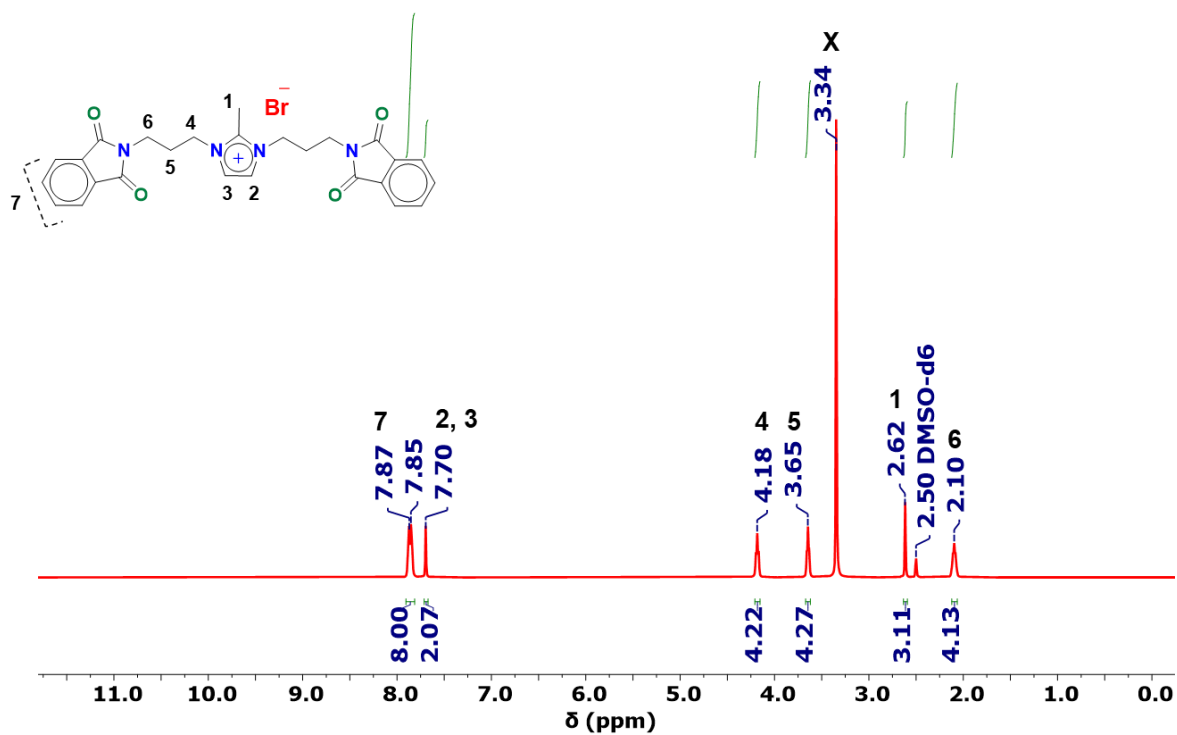


Figure S3.  $^1\text{H}$  NMR spectrum of **9** in  $\text{DMSO}-d_6$ , X:  $\text{H}_2\text{O}$ .

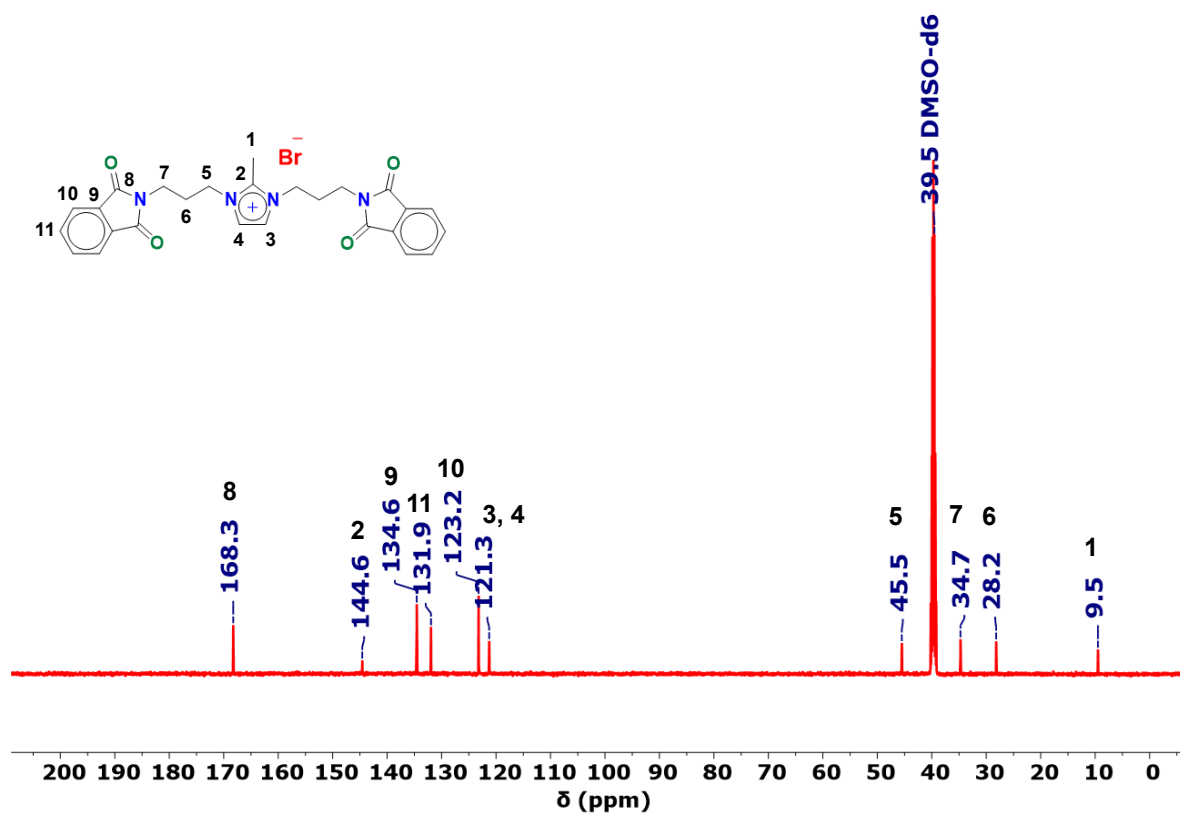


Figure S4.  $^{13}\text{C}$  NMR spectrum of **9** in DMSO- $d_6$ .

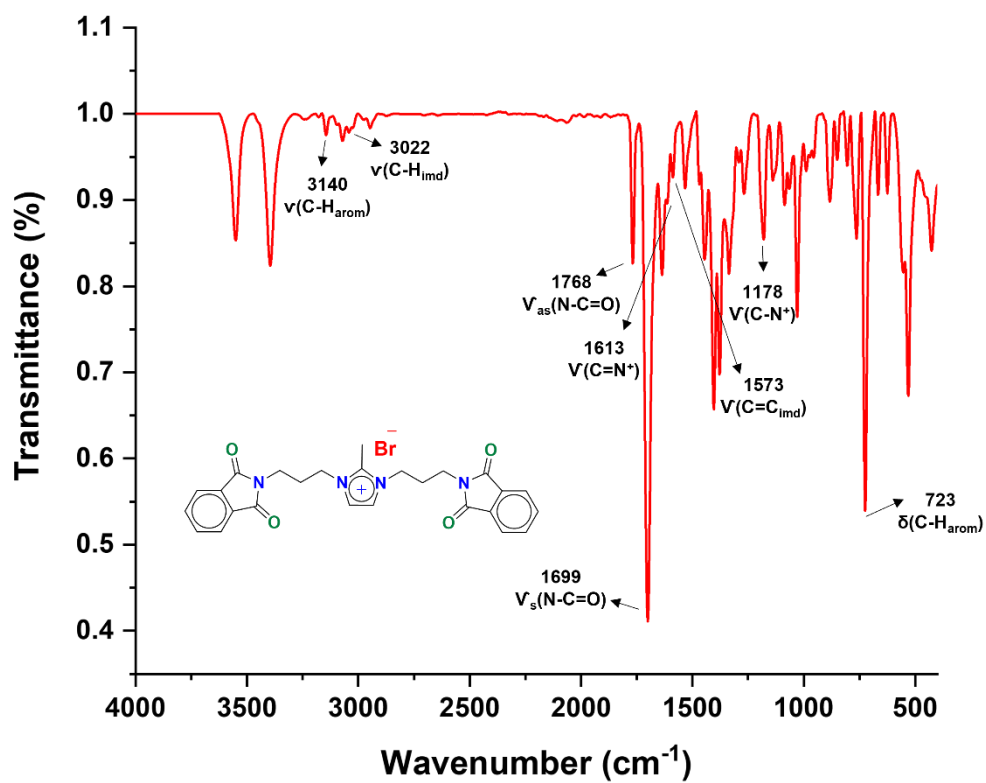
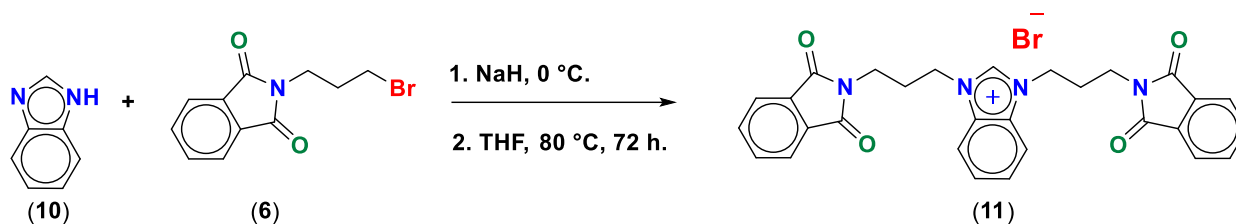


Figure S5. ATR-FTIR spectrum of **9**.

### 1.3 1,3-bis(3-(1,3-dioxoisindolin-2-yl)propyl)-1*H*-benzo[*d*]imidazol-3-ium bromide (**11**)



**Scheme S2.** Synthetic route of 1,3-bis(3-(1,3-dioxoisindolin-2-yl)propyl)-1*H*-benzo[*d*]imidazol-3-ium bromide (**11**).

Based on the aforementioned method discussed in section **1.2**, 1,3-bis(3-(1,3-dioxoisindolin-2-yl)propyl)-1*H*-benzo[*d*]imidazol-3-ium bromide (**11**) was synthesized using benzimidazole (**10**, 1.156 g, 9.59 mmol), NaH (0.42 g, 10.55 mmol, 1.1 *eq.*), N-(3-bromopropyl)phthalimide (**6**, 5.77 g, 21.52 mmol, 2.2 *eq.*). The workup includes filtration, washing the precipitate with 100 mL as-received THF, and recrystallized using hot EtOH. For further crops isolation, the yellow filtrate was evaporated, and treated with the as-received THF with continuous stirring. The second crop purified followed the same procedure with a total yield of 45%. **EA** (C<sub>29</sub>H<sub>25</sub>N<sub>4</sub>O<sub>4</sub>Br; Calculated (%): C, 60.74; H, 4.39; N, 9.77. Found (%): C, 60.86; H, 4.44; N, 9.74). **HRMS** (*m/z* of [C<sub>29</sub>H<sub>25</sub>N<sub>4</sub>O<sub>4</sub><sup>+</sup>], Calculated: 493.18703. Found: 493.19856). Melting point = 234 °C.

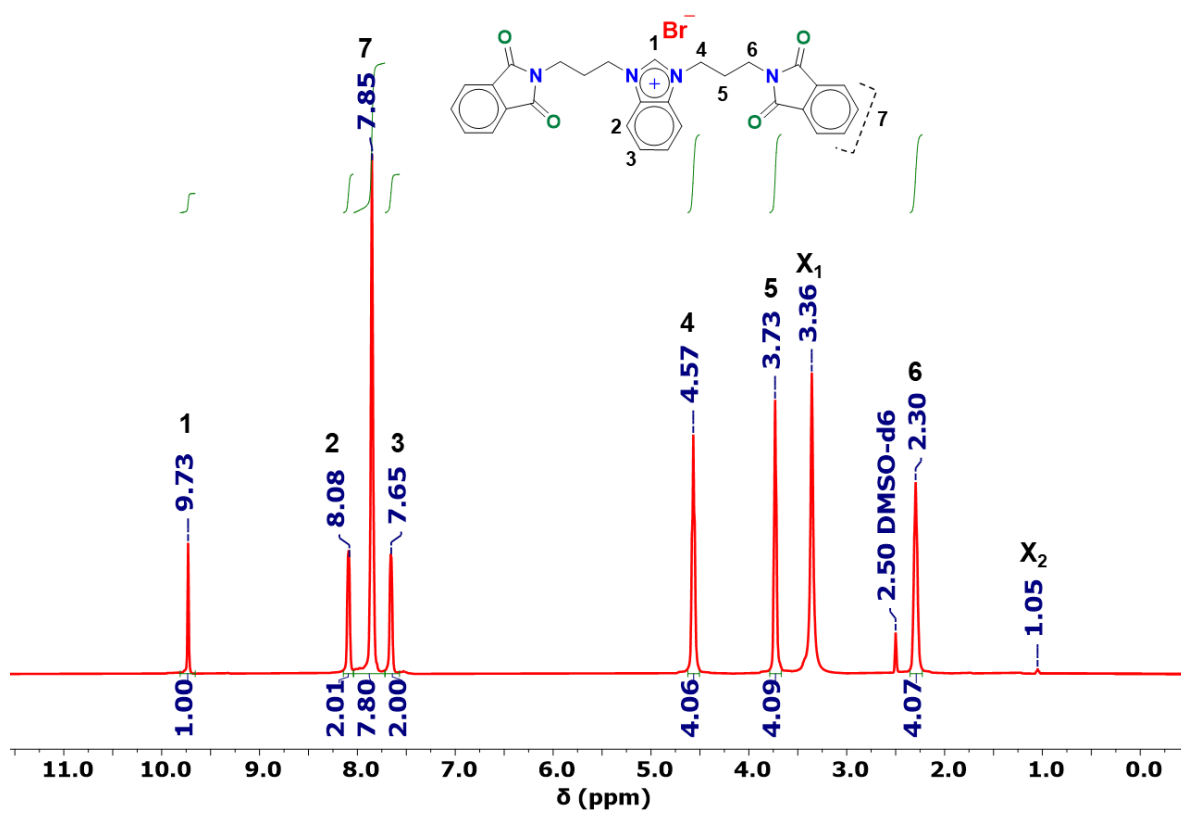


**Figure S6.**  $^1\text{H}$  NMR spectrum of **11** in  $\text{DMSO-}d_6$ , X<sub>1</sub>:  $\text{H}_2\text{O}$ , X<sub>2</sub>: grease.



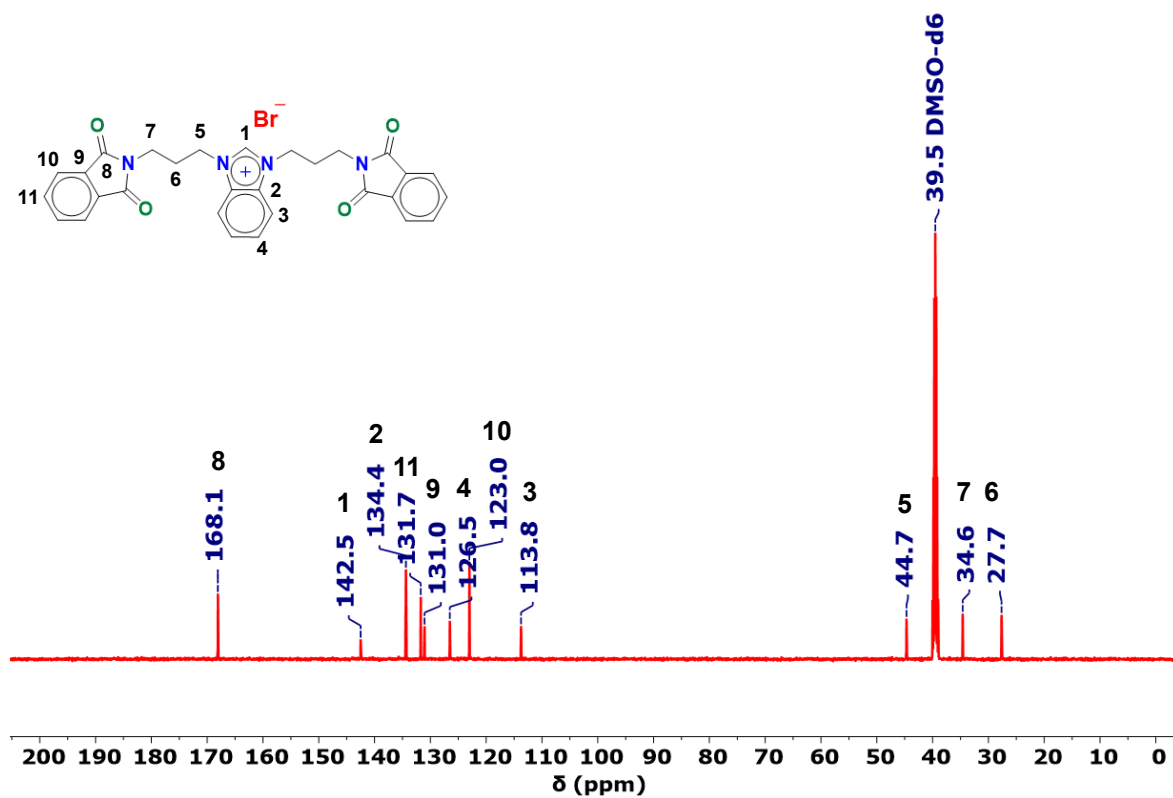


Figure S7.  $^{13}\text{C}$  NMR spectrum of **11** in  $\text{DMSO}-d_6$ .

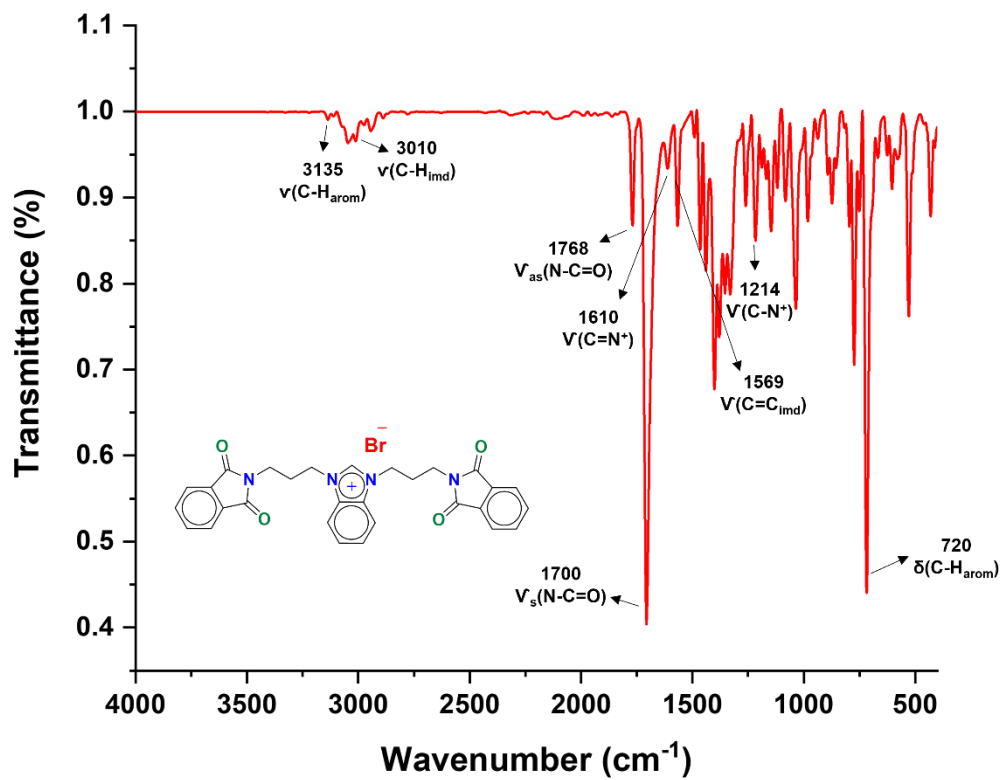
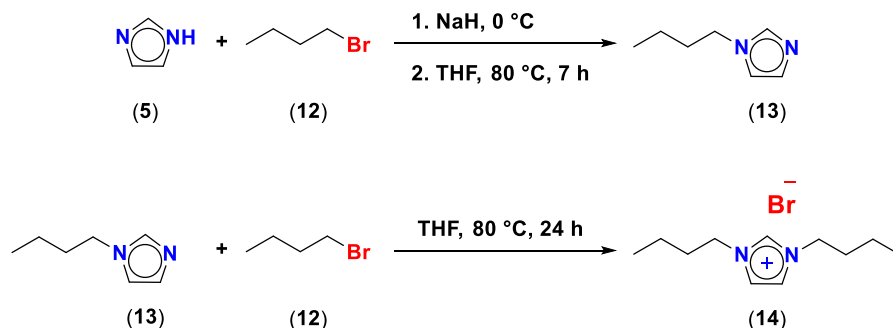


Figure S8. ATR-FTIR spectrum of **11**.

#### 1.4 1,3-dibutyl-1*H*-imidazol-3-ium bromide (**14**)



**Scheme S3.** Synthetic route of 1,3-dibutyl-1*H*-imidazol-3-ium bromide (**14**).

Following the same procedure used to synthesize **9** (Section 2.1), **13** was synthesized using a mixture of imidazole (**5**, 1.30 g, 19.14 mmol), NaH (0.55 g, 22.97 mmol, 1.2 *eq.*), bromobutane (**12**, 3.15 g, 22.97 mmol, 2.2 *eq.*). The mixture was refluxed for 7 h. The product was filtered and washed with 100 mL, as-received THF. The filtrate evaporated and the resulting yellow liquid was treated with 50 mL of DCM. The solution cooled in the freezer for 1 h, and the resulting solid was filtered out. The solvent was evaporated while the crude syrup was washed with 100 mL of diethyl ether, cooled in the freezer till the next day, and filtered using a nylon filter paper. **13** was isolated after evaporating the solvent and dried under vacuum for 1 h at 90 °C. After that, 1,3-dibutyl-1*H*-imidazol-3-ium bromide (**14**) was synthesized upon a dropwise addition of a solution of **12** (5.2 mL, 48.3 mmol, 4 *eq.*), to a solution of **13** prepared in 10 and 40 mL, respectively of the as-received THF. Upon mixing, the solution was refluxed for 24 h with continuous stirring with an isolated prominent layer. The latter was separated by extraction from the reaction mixture followed by another extraction with 20 mL as-received THF and dried under vacuum for 1 h at 90 °C. Yield: 38%.

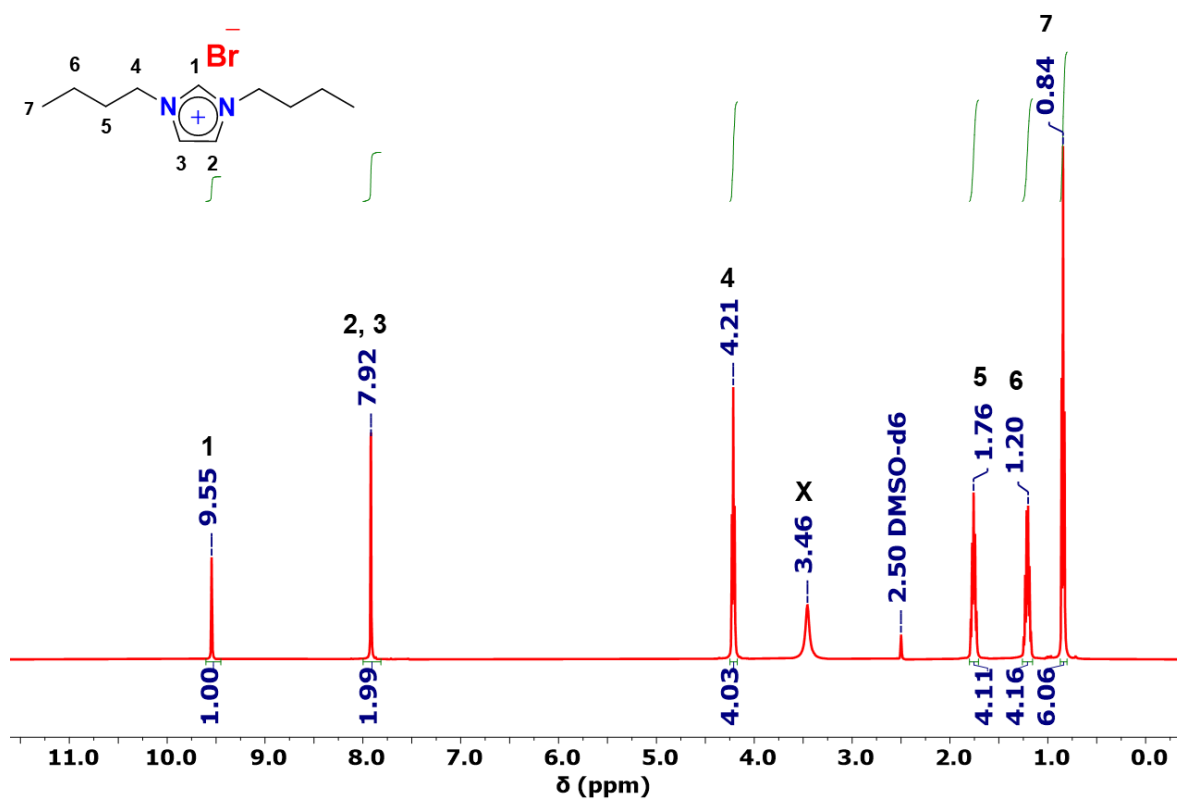


Figure S9.  $^1\text{H}$  NMR spectrum of **14** in DMSO- $d_6$ , X: H<sub>2</sub>O.

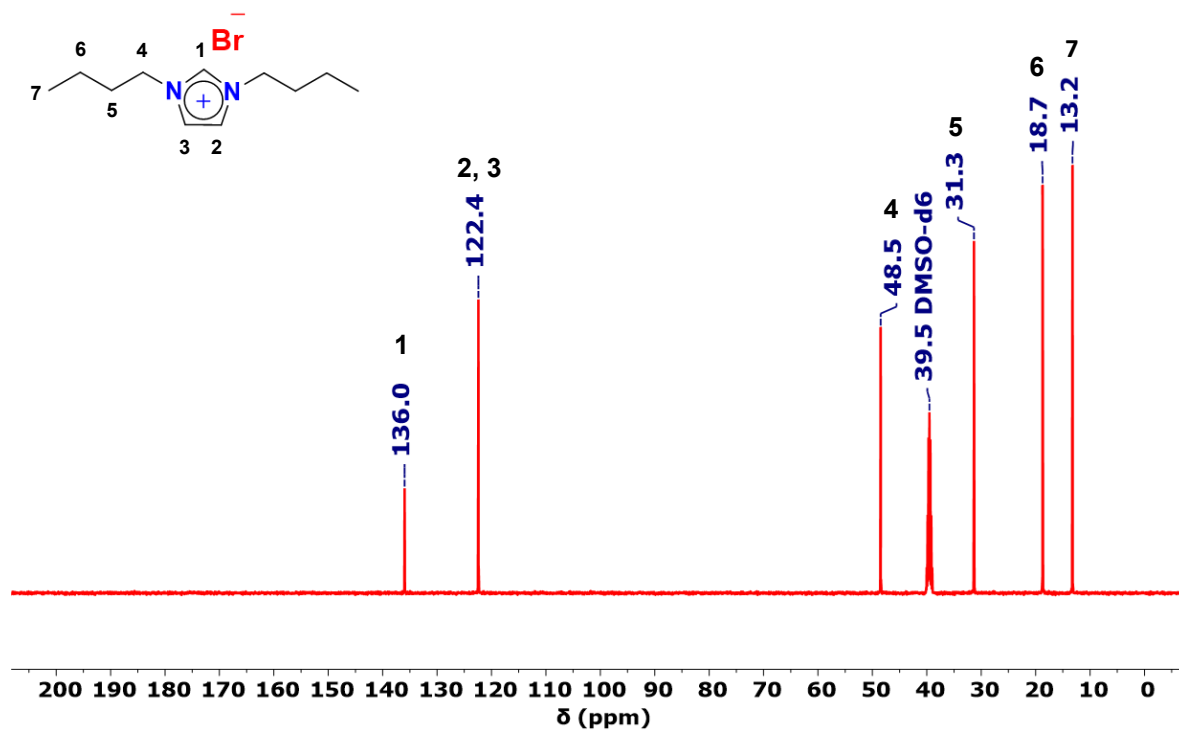


Figure S10. <sup>13</sup>C NMR spectrum of **14** in DMSO-*d*<sub>6</sub>.

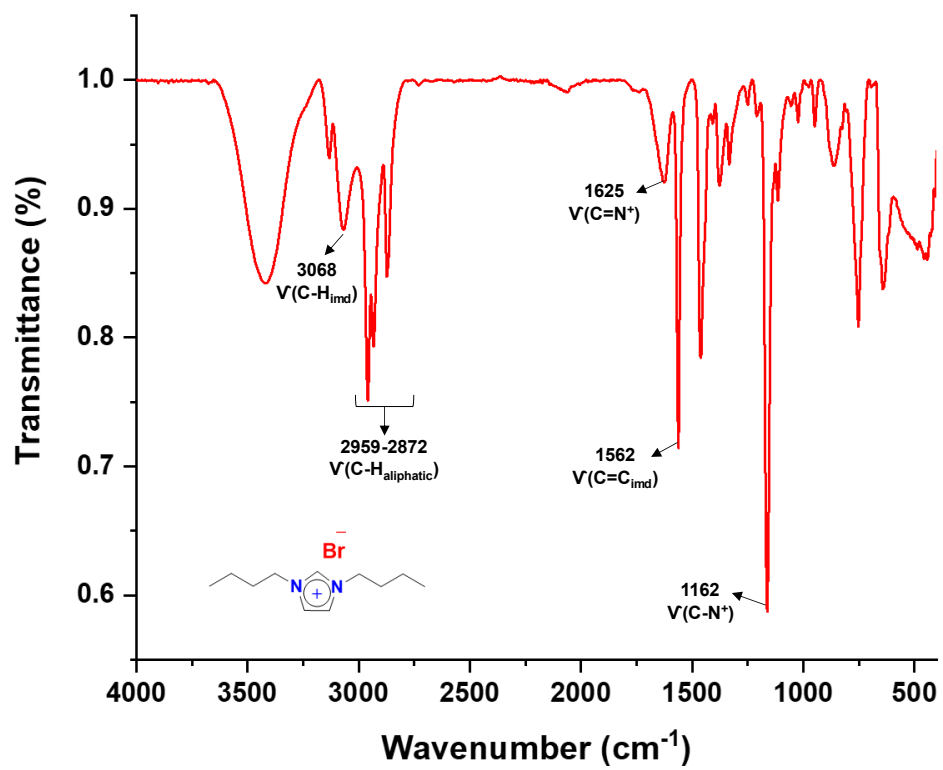
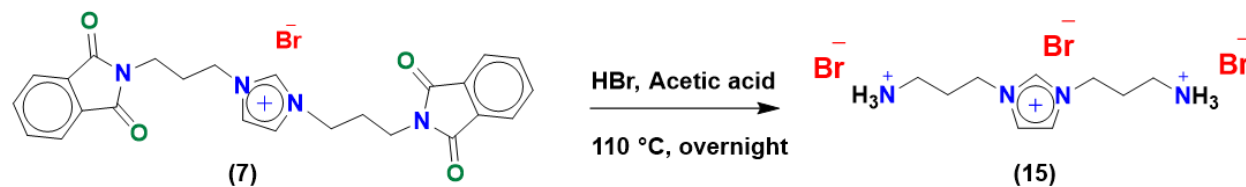


Figure S11. ATR-FTIR spectrum of 14.

### 1.5 1,3-bis(3-ammoniopropyl)-1*H*-imidazol-3-ium bromide (**15**)



**Scheme S4.** Synthetic route of 1,3-bis(3-ammoniopropyl)-1*H*-imidazol-3-ium bromide (**15**).

Following the published procedure:<sup>1</sup> A TSIL precursor (**7**, 2.50 g, 4.78 mmol) was dissolved in a mixture of glacial acetic acid (11.2 mL) and HBr (11.2 mL). The solution was refluxed at 110 °C overnight, cooled to RT, the white crystal of phthalic acid was filtered out and washed with 15 mL of EtOH, where the filtrate was placed in the freezer till the next day to get rid of any traces of phthalic acid as much as possible. The filtrate was filtered once again and evaporated to get a concentrated orange solution (about 10 mL), then treated with 30 mL of acetone to get a white solid (**15**), which was filtered out and washed with diethyl ether. For the single crystal-XRD measurement, part of the solution was placed at -20 °C for 1 month to form a white needle crystal. Yield: 63%. EA (C<sub>9</sub>H<sub>21</sub>N<sub>4</sub>Br<sub>3</sub>; Calculated (%): C, 25.43; H, 4.98; N, 13.18. Found (%): C, 25.51; H, 4.92; N, 13.01). Melting point = 217 °C.

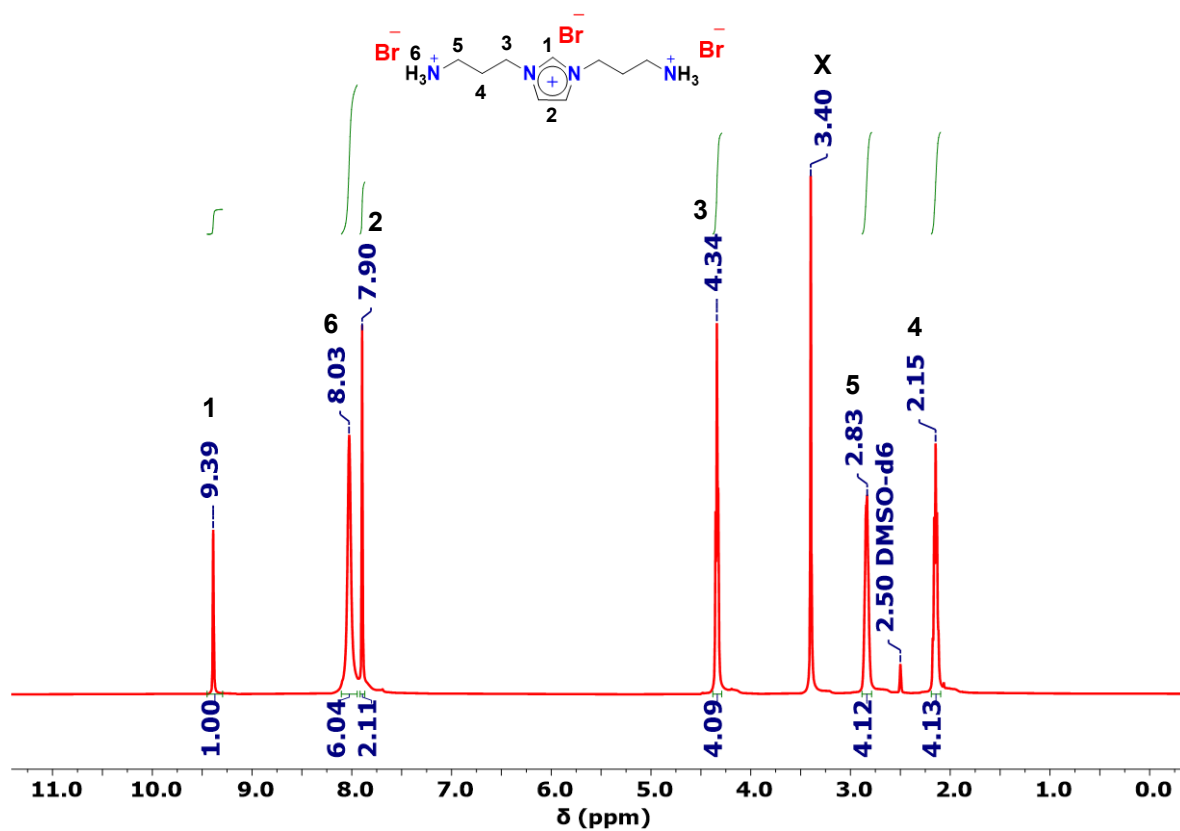


Figure S12.  $^1\text{H}$  NMR spectrum of **15** in  $\text{DMSO-}d_6$ , X:  $\text{H}_2\text{O}$ .



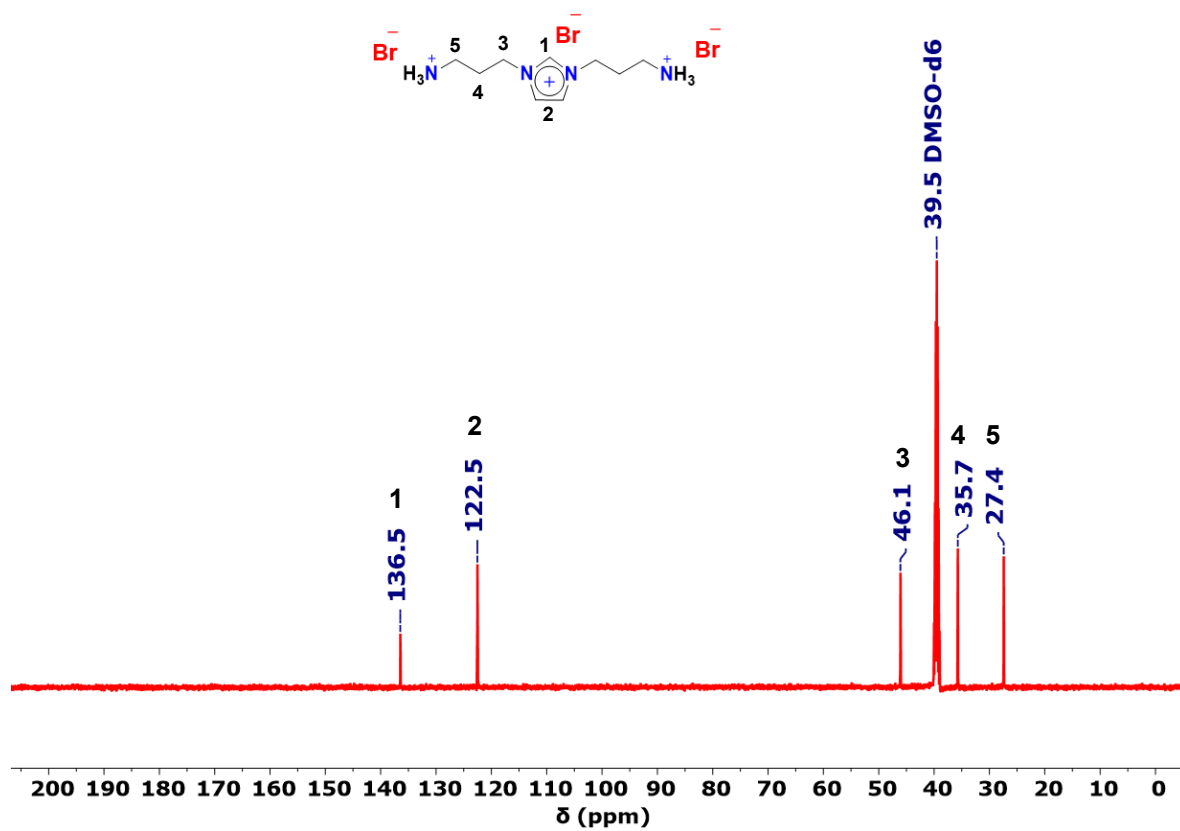
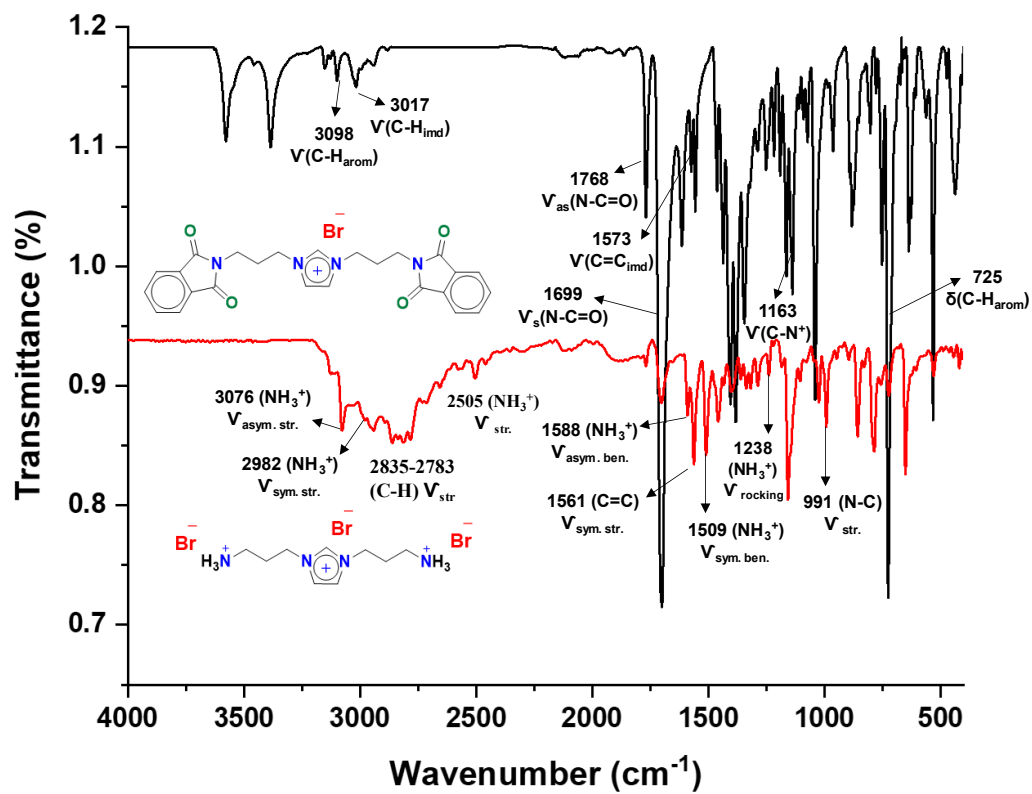
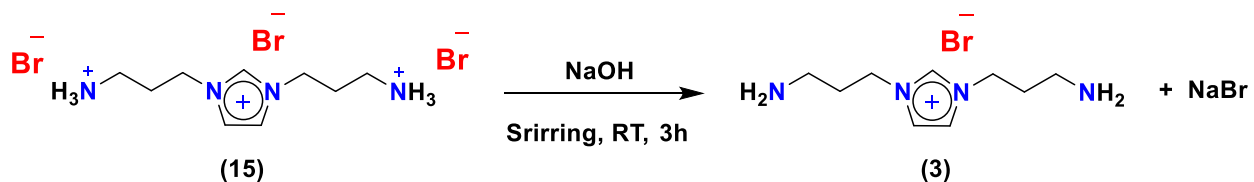


Figure S13.  $^{13}\text{C}$  NMR spectrum of **15** in DMSO- $d_6$ .



**Figure S14.** ATR-FTIR spectra of 1,3-bis(3-ammoniopropyl)-1*H*-imidazol-3-ium bromide (**15**, red traces) and 1,3-bis(3-(1,3-dioxoisindolin-2-yl)propyl)-1*H*-imidazol-3-ium bromide (**7**, black traces).

## 1.6 1,3-bis(3-aminopropyl)-1*H*-imidazol-3-ium bromide (**3**)



**Scheme S5.** Synthetic route of 1,3-bis(3-aminopropyl)-1*H*-imidazol-3-ium bromide (**3**).

In a 50 mL round-bottomed flask equipped with a magnetic stirring bar, a solution of NaOH pellet in 2 mL of distilled water (0.047 g, 1.97 mmol, 2 *eq.*) was added to a solution of **15** (0.42 g, 0.985 mmol) in 10 mL of EtOH, which was left to stir for 3 h at RT, a pale-yellowish solution is observed when the mixing time is over. The solid NaBr was filtered out, and the solvent was evaporated. The target product was obtained with some traces of NaBr so the process of washing with EtOH was repeated to eliminate NaBr.

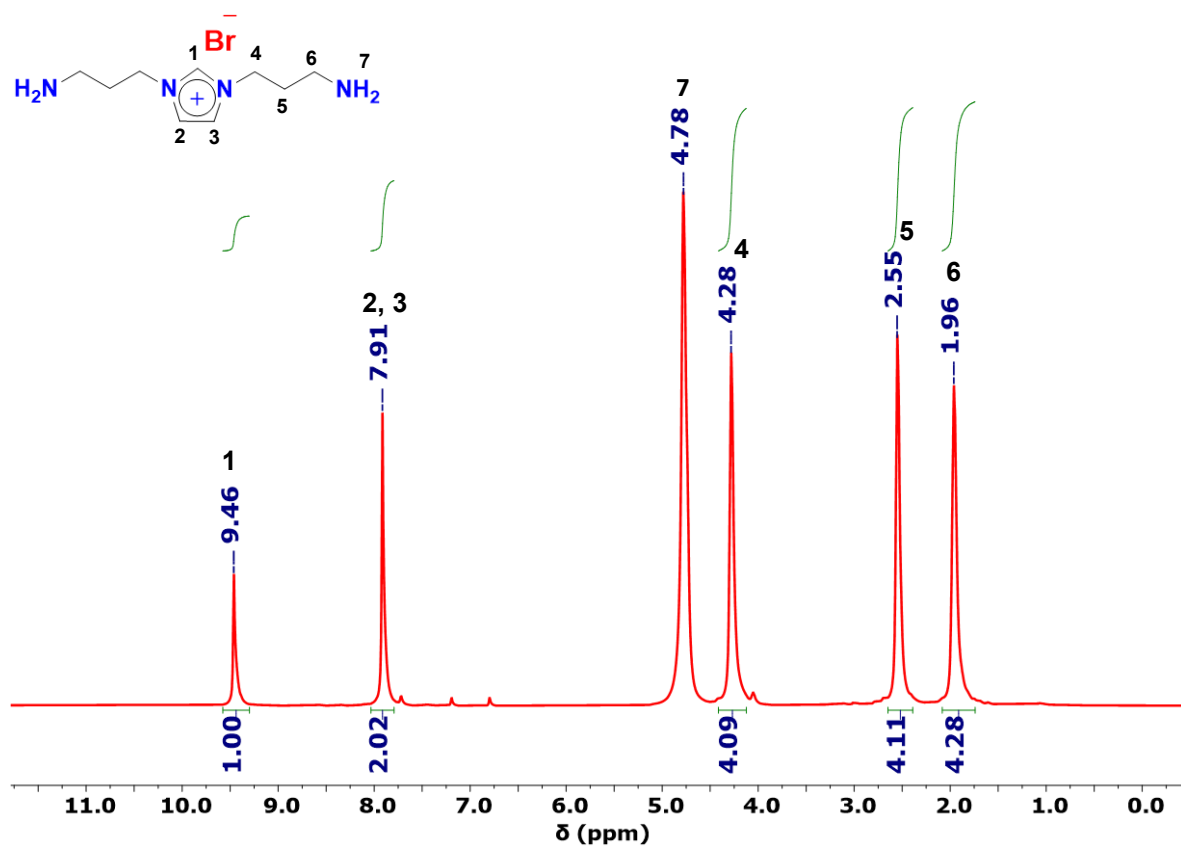


**Figure S15.**  $^1\text{H}$  NMR spectrum of **3** in  $\text{DMSO}-d_6$ .

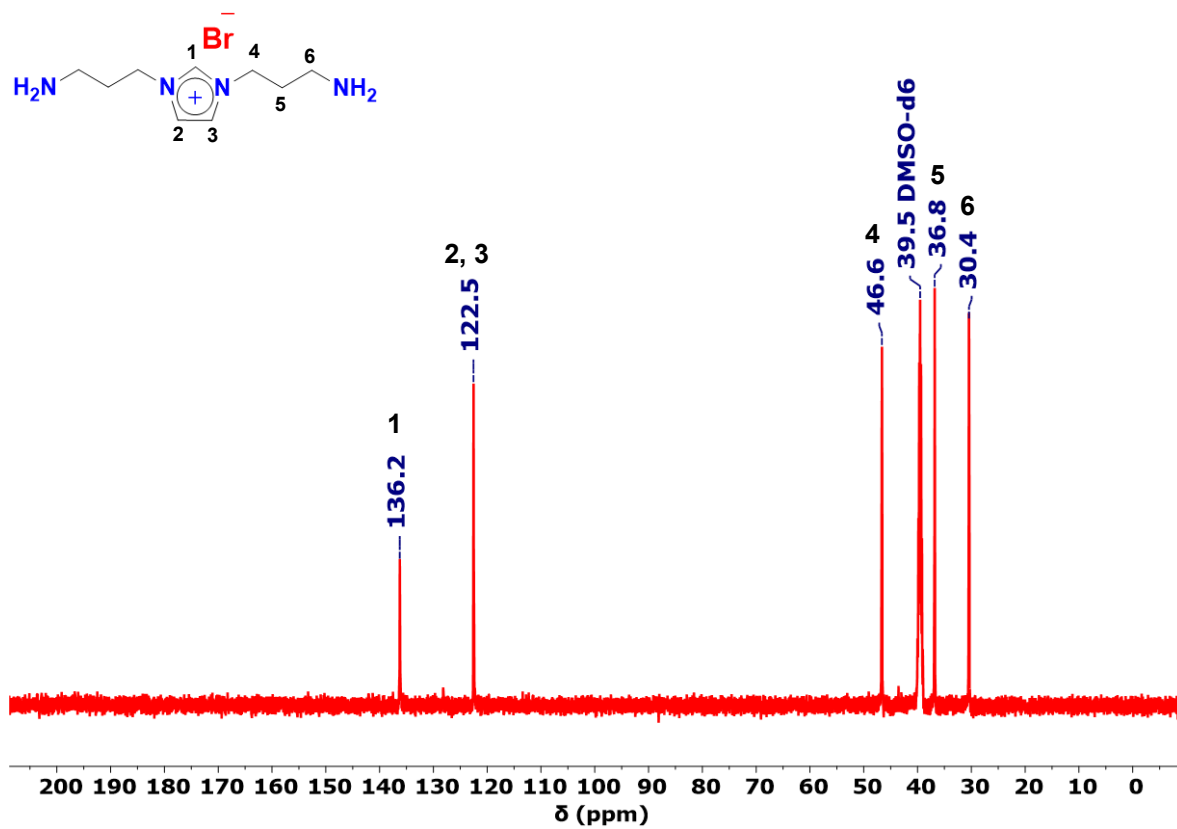
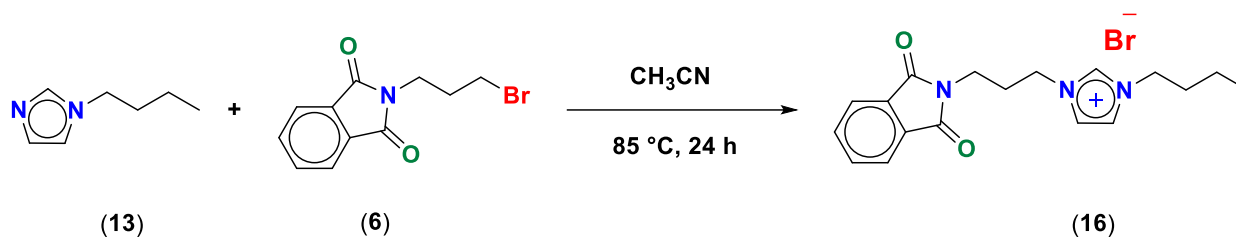


Figure S16.  $^{13}\text{C}$  NMR spectrum of **3** in  $\text{DMSO-}d_6$ .

### 1.7 1-butyl-3-(3-(1,3-dioxisoindolin-2-yl)propyl)-1*H*-imidazol-3-ium bromide (**16**)



**Scheme S6.** Synthetic route of 1-butyl-3-(3-(1,3-dioxisoindolin-2-yl)propyl)-1*H*-imidazol-3-ium bromide (**16**).

In a 100 mL round-bottomed flask equipped with a magnetic stirring bar, a solution of **13**, 1.10 g, 8.85 mmol) was dissolved in 25 mL of acetonitrile, then the prepared solution of **6**, 3.44 g, 12.8 mmol) in 25 mL of acetonitrile was added dropwise to the previous solution and refluxed at 85 °C for 24 h. Afterward, the white precipitate was filtered out, washed with 50 mL of acetonitrile, and dried. Yield: 60%. **EA** (C<sub>18</sub>H<sub>22</sub>N<sub>3</sub>O<sub>2</sub>Br; Calculated (%): C, 55.11; H, 5.65; N, 10.71. Found (%): C, 55.19; H, 5.85; N, 10.54). **HRMS** ( $m/z$  of [C<sub>29</sub>H<sub>25</sub>N<sub>4</sub>O<sub>4</sub>]<sup>+</sup>, Calculated: 312.17065; Found: 312.17468). Melting point = 136 °C.

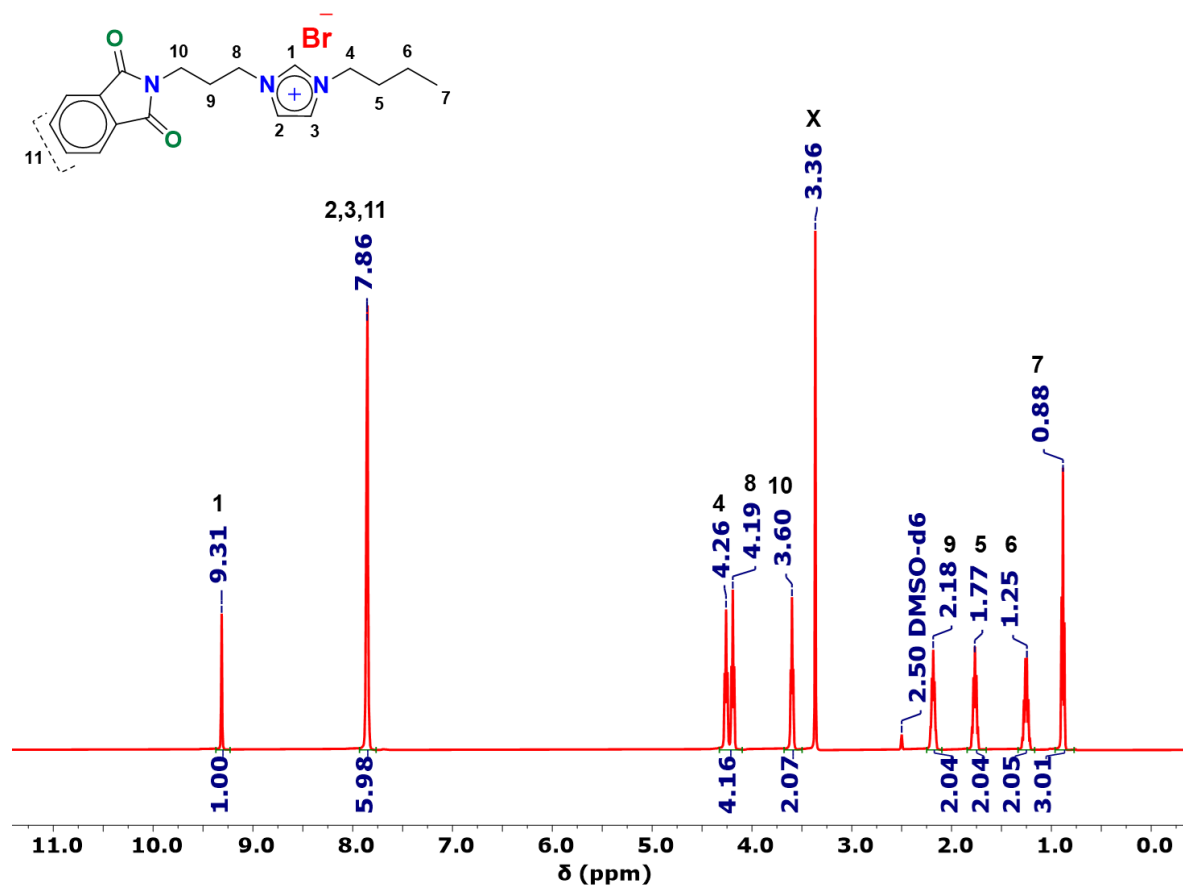


Figure S17.  $^1\text{H}$  NMR spectrum of **16** in DMSO- $d_6$ , X: H<sub>2</sub>O.

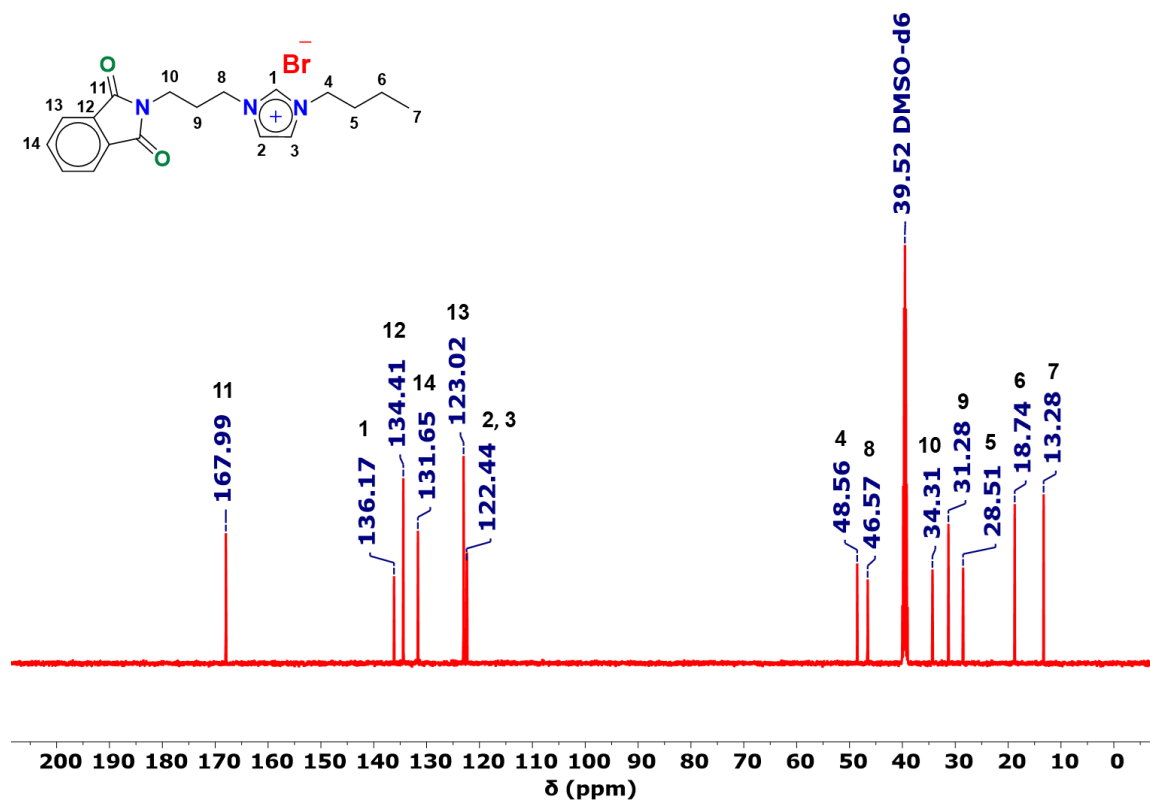


Figure S18.  $^{13}\text{C}$  NMR spectrum of **16** in DMSO- $d_6$ .



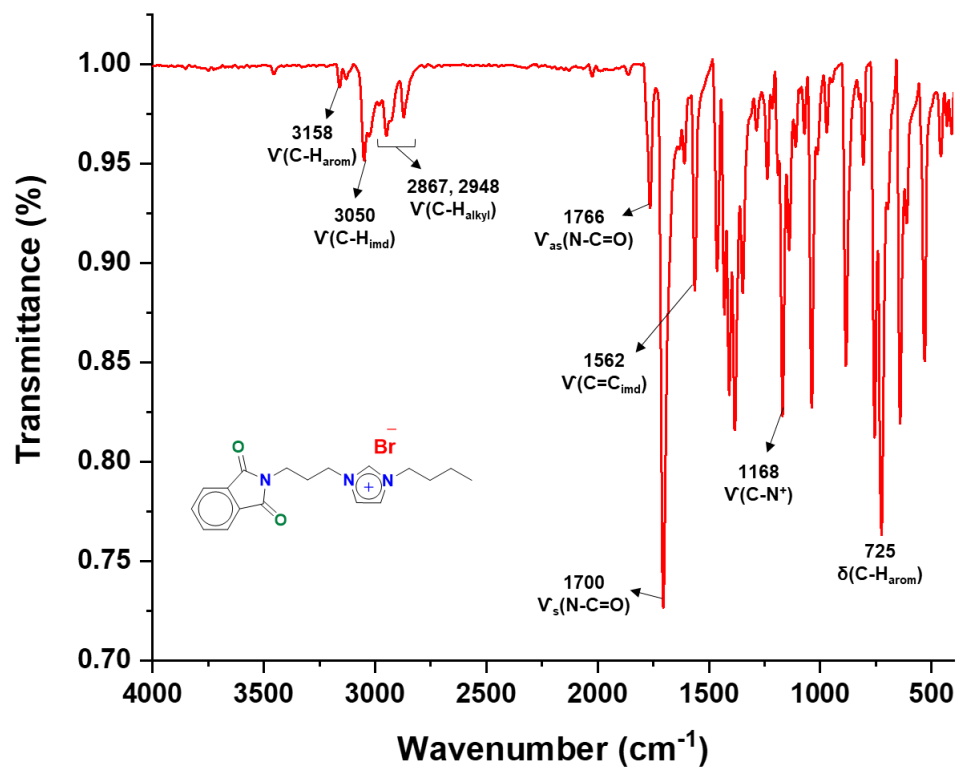
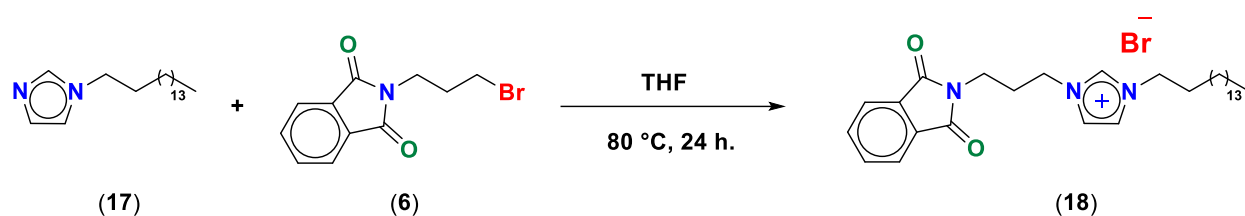


Figure S19. ATR-FTIR spectrum of 16.

### 1.8 3-(3-(1,3-dioxoisindolin-2-yl)propyl)-1-hexadecyl-1*H*-imidazol-3-ium bromide (**18**)



**Scheme S7.** Synthetic route of 3-(3-(1,3-dioxoisindolin-2-yl)propyl)-1-hexadecyl-1*H*-imidazol-3-ium bromide (**18**).

In a 100 mL round-bottomed flask equipped with a magnetic stirring bar, the solution of (**6**, 1.075 g, 4.01 mmol) in 20 mL of as-received THF was added dropwise to the solution of (**17**, 0.782 g, 2.67 mmol) in 20 mL of as-received THF (N-hexadecyl imidazole, **17** was prepared following a literature procedure)<sup>2</sup>. Afterward, the reaction was refluxed for 24 h at 80 °C. Then, a white precipitate was filtered out, washed with 50 mL of as-received THF, and dried. Yield: 67%. **HRMS** ( $m/z$  of [C<sub>30</sub>H<sub>46</sub>N<sub>3</sub>O<sub>2</sub>]<sup>+</sup>, Calculated: 480.35845. Found: 480.36773). Melting point = 160 °C.

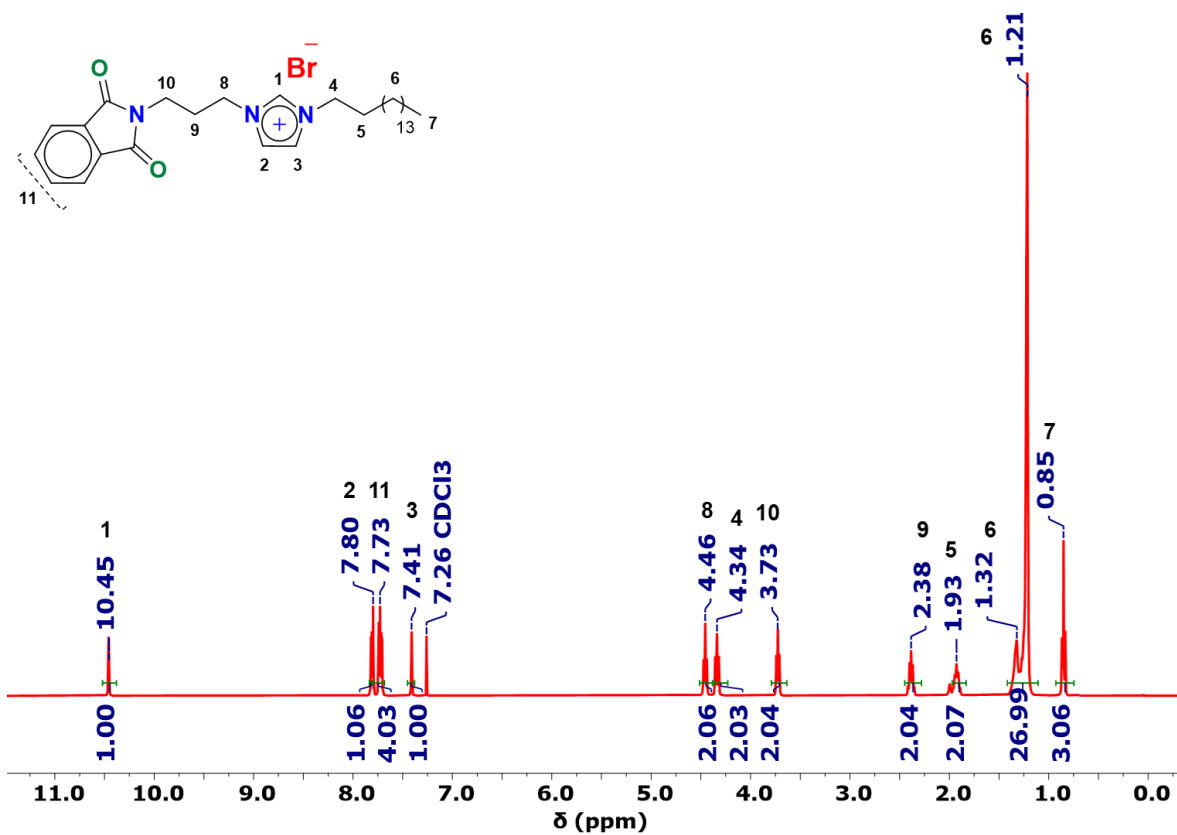


Figure S20. <sup>1</sup>H NMR spectrum of **18** in CDCl<sub>3</sub>.

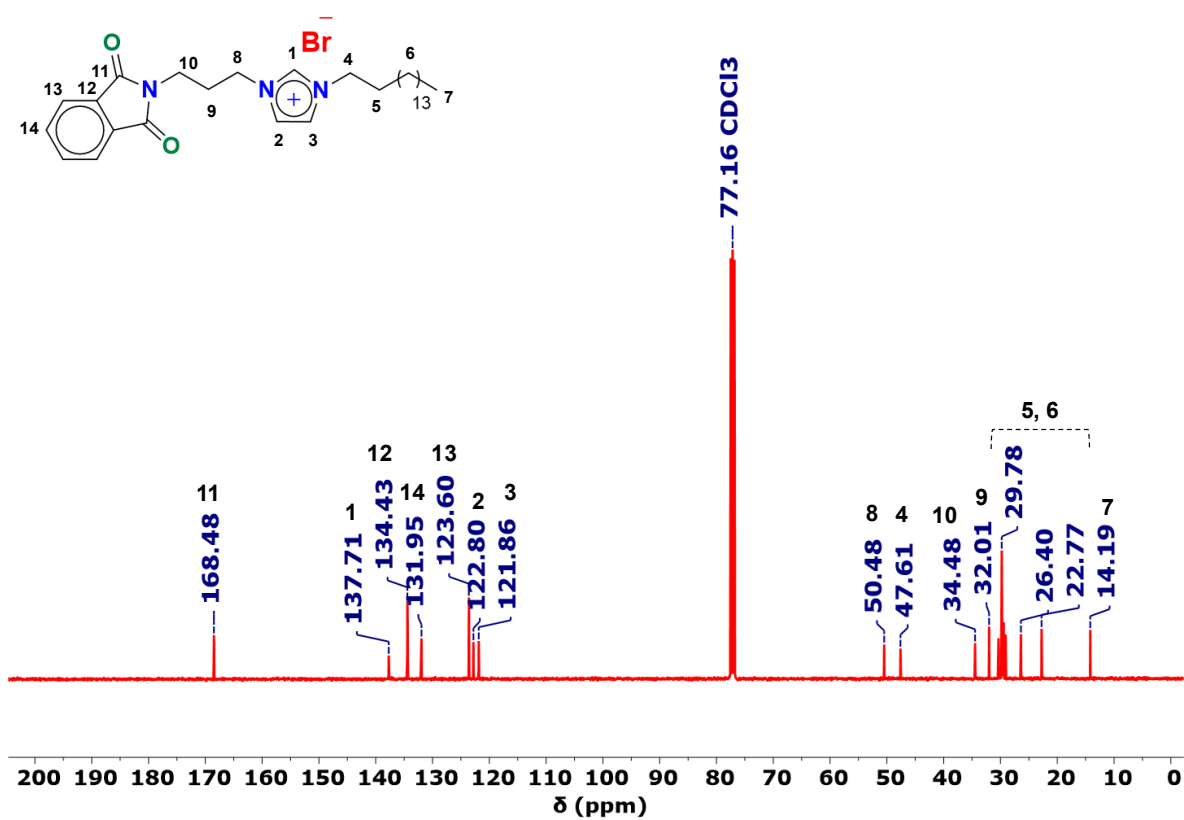


Figure S21. <sup>13</sup>C NMR spectrum of **18** in CDCl<sub>3</sub>.

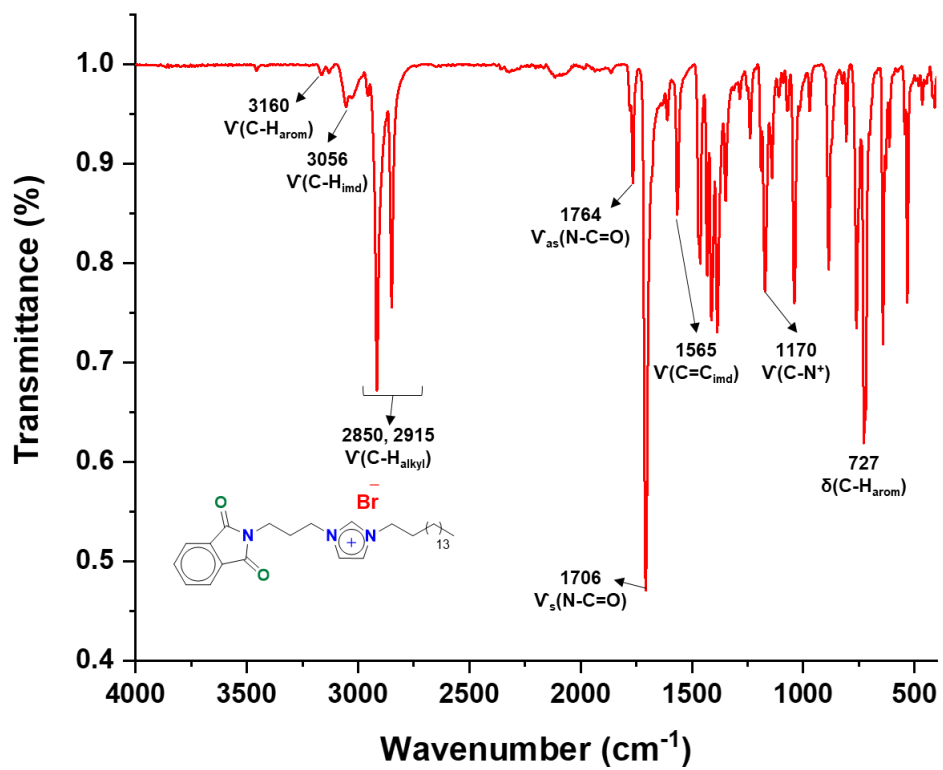
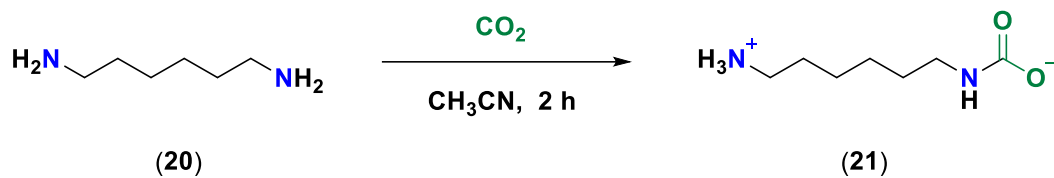


Figure S22. ATR-FTIR spectrum of **18**.

### 1.9 6-ammoniumhexylenecarbamate (21)



**Scheme S8.** Synthetic route to produce **21**.

In a 100 mL round-bottomed flask equipped with a magnetic stirring bar, 1,6-hexanediamine (**20**, 1.30 g, 11.18 mmol) was dissolved in 60 mL of acetonitrile, then bubbled with CO<sub>2</sub> for 2 h at RT. A white precipitate was filtered out, washed with 20 mL of acetonitrile, and dried under vacuum for 8 h.

## 2 Thermal Gravimetric Analysis (TGA)

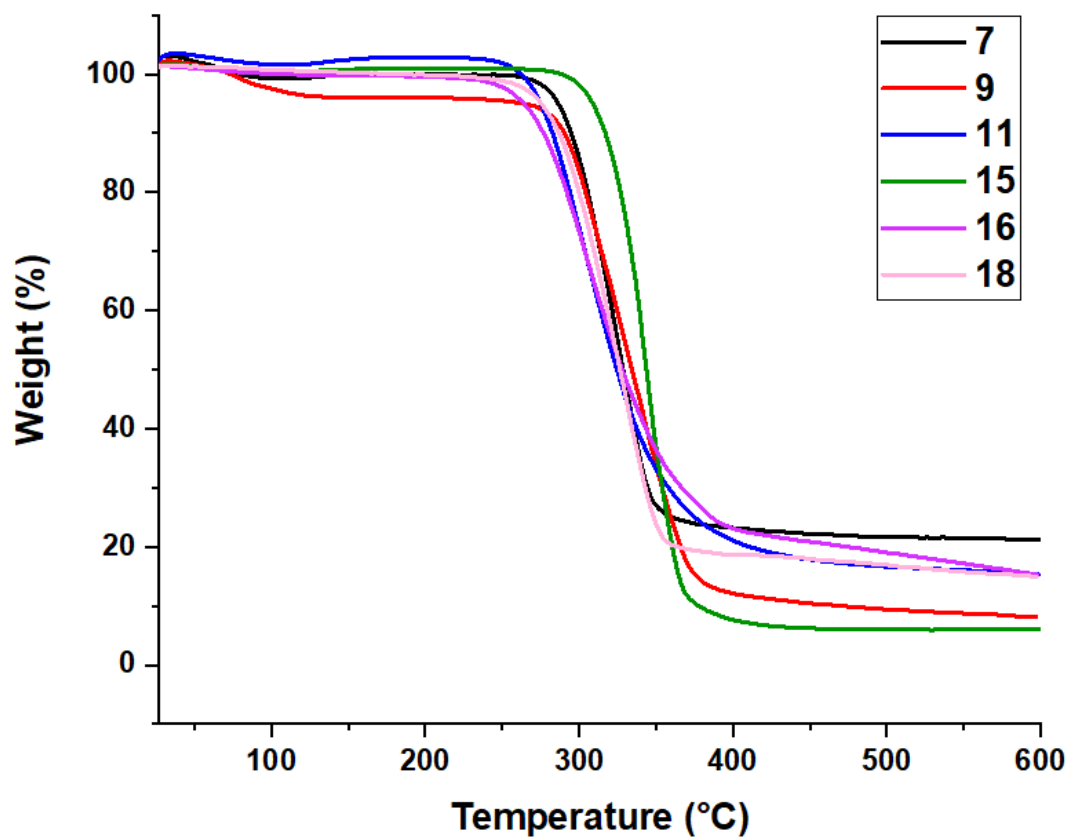


**Figure S23.** TGA traces of imidazolium derivatives [7 (black trace), 9 (red trace), 11 (blue trace), 15 (green trace), 16 (purple trace), and 18 (pink trace)].

### 3 Cycloaddition reaction

#### 3.1 Time Profile

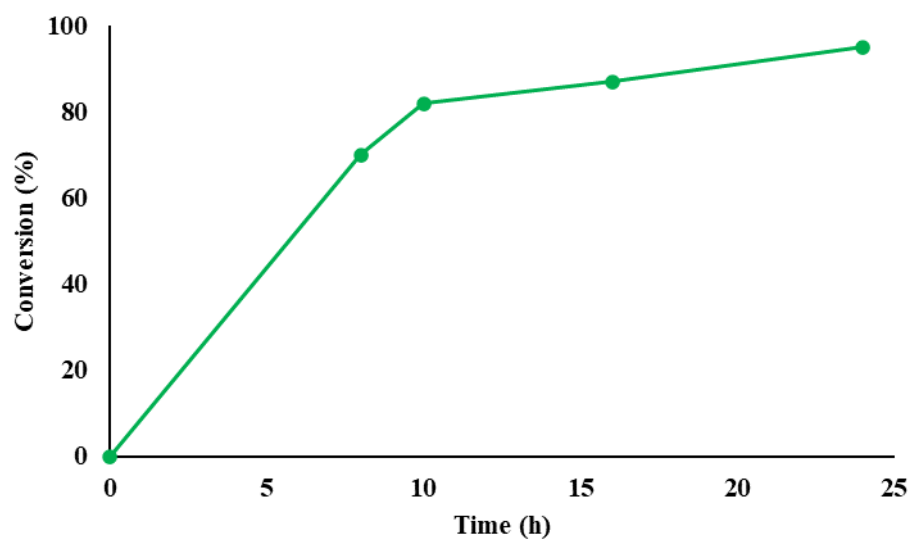


**Figure S24.** Reaction time profile for the conversion of ECH (1 mL) at 90 °C in DMSO (0.5 ml) using 3 mol% of **7** under atmospheric CO<sub>2</sub> pressure. Representative <sup>1</sup>H NMR spectrum for each entry is shown in Figure S26-S29.



### 3.2 $^1\text{H}$ NMR spectra of Cyclic Carbonates (CCs) reaction

For reproducibility purposes, two experiments of each desired carbonate were performed, and percent conversion was calculated and listed as an average conversion of both experiments.

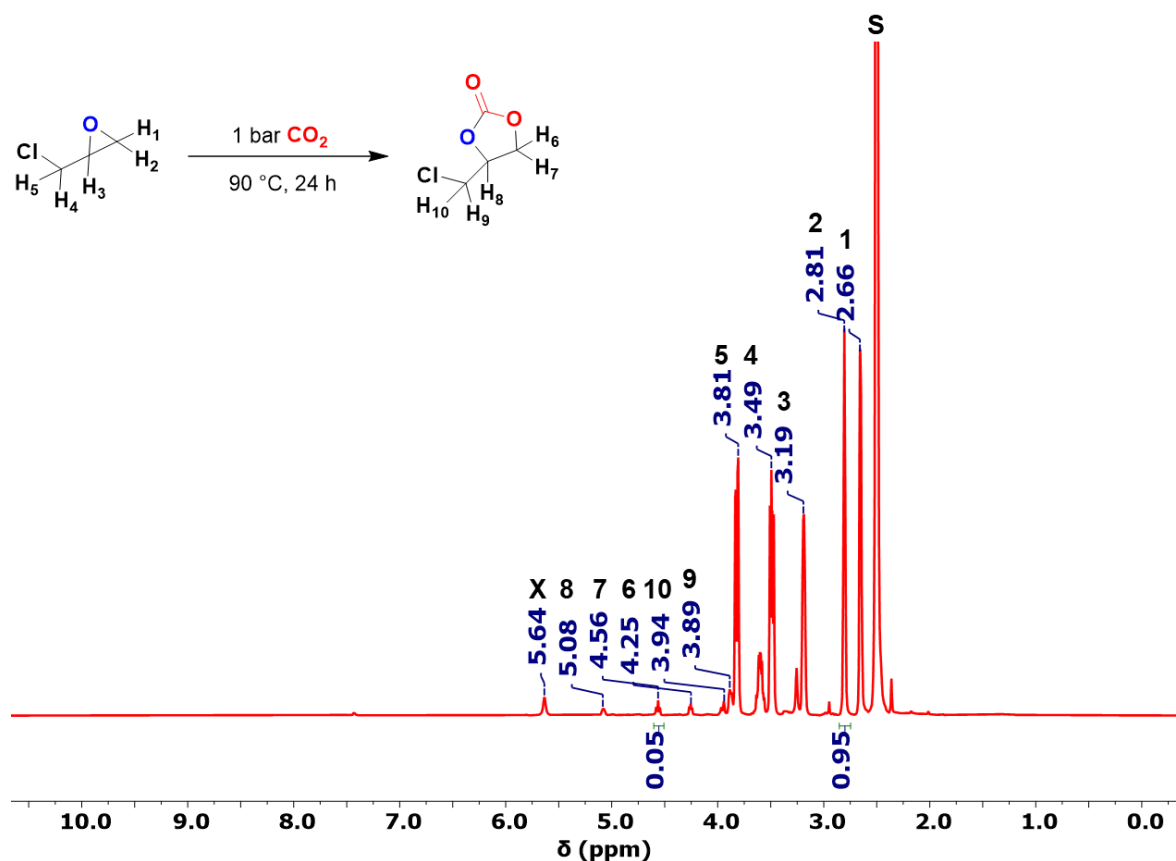


**Figure S25.**  $^1\text{H}$  NMR spectrum of the conversion of ECH into its corresponding carbonate in  $\text{DMSO}-d_6$ , S: solvent, X: 3-chloropropane-1,2-diol (found in the original sample as supplied by the chemical vendor).

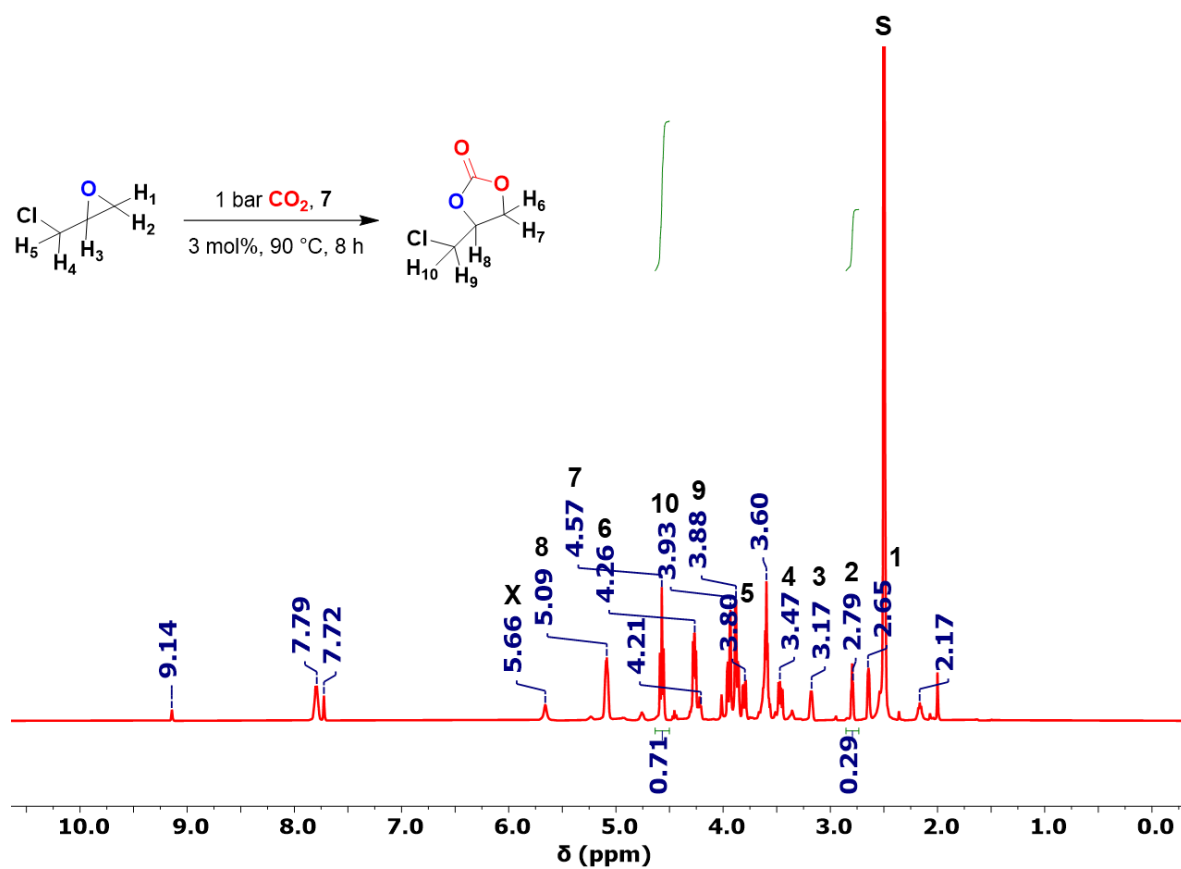


**Figure S26.**  $^1\text{H}$  NMR spectrum of the conversion of ECH into its corresponding carbonate in  $\text{DMSO}-d_6$ , S: solvent, X: 3-chloropropane-1,2-diol (from the starting material as supplied by the chemical vendor), peaks at 2.17, 3.60, 4.21, 7.72, 7.79, and 9.14 ppm correspond to the catalyst.

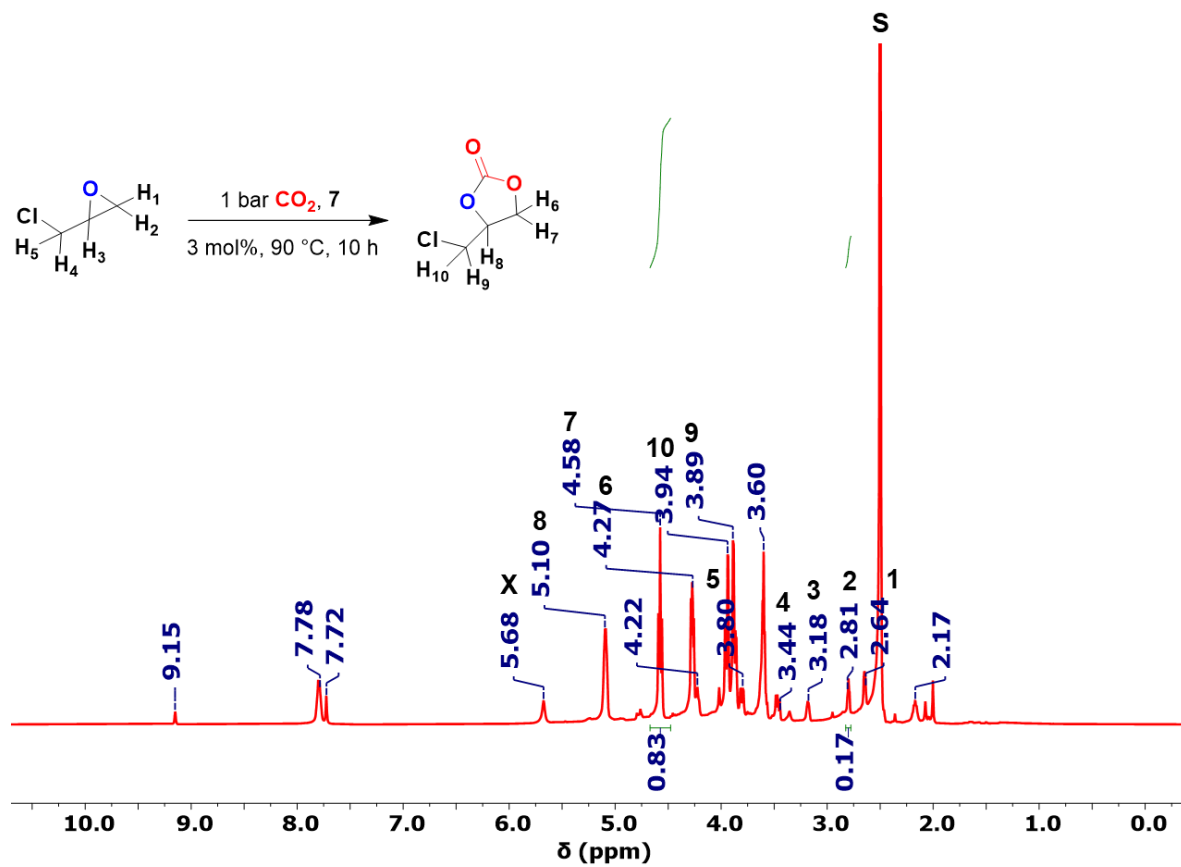


**Figure S27.**  $^1\text{H}$  NMR spectrum of the conversion of ECH into its corresponding carbonate in  $\text{DMSO-}d_6$ , S: solvent, X: 3-chloropropane-1,2-diol (from the starting material as supplied by the chemical vendor), peaks at 2.17, 3.60, 4.22, 7.72, 7.78, and 9.15 ppm correspond to the catalyst.

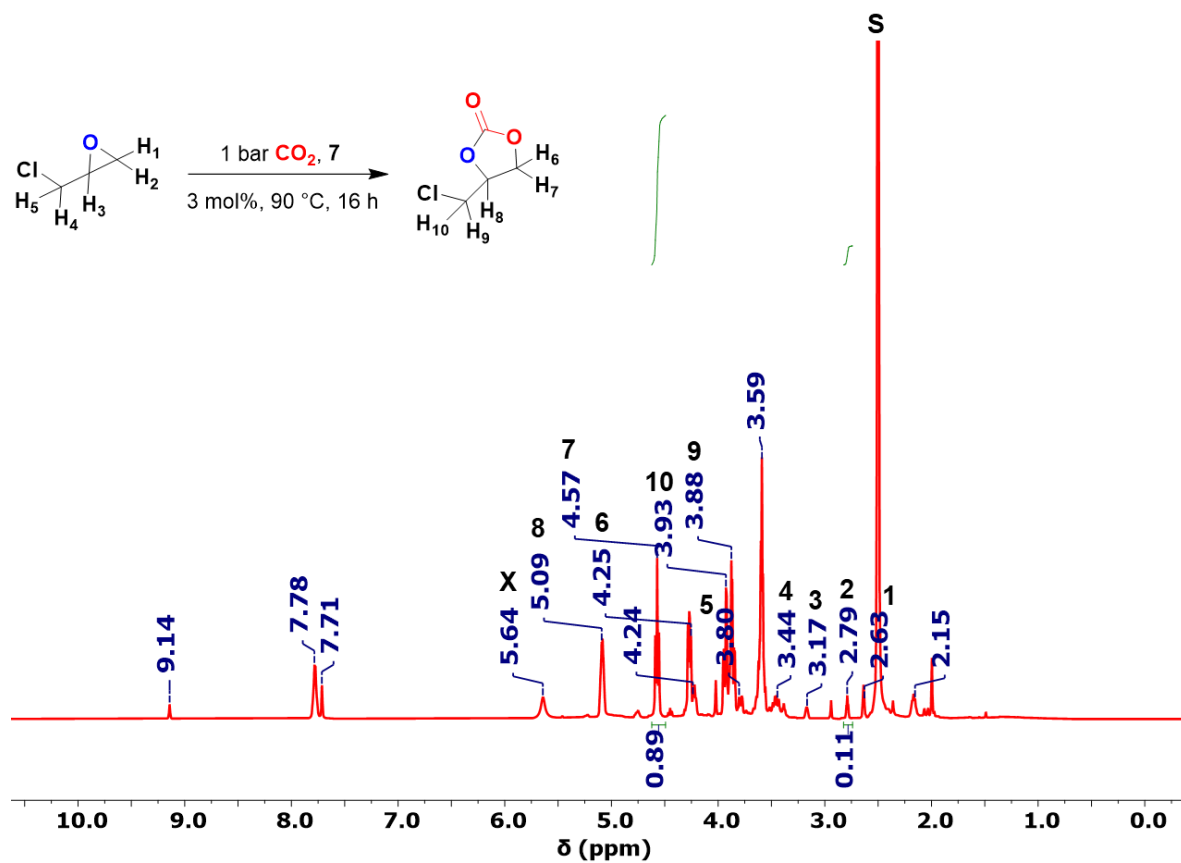


**Figure S28.**  $^1\text{H}$  NMR spectrum of the conversion of ECH into its corresponding carbonate in DMSO- $d_6$ , S: solvent, X: 3-chloropropane-1,2-diol (from the starting material as supplied by the chemical vendor), peaks at 2.15, 3.59, 4.24, 7.71, 7.78, and 9.14 ppm correspond to the catalyst.

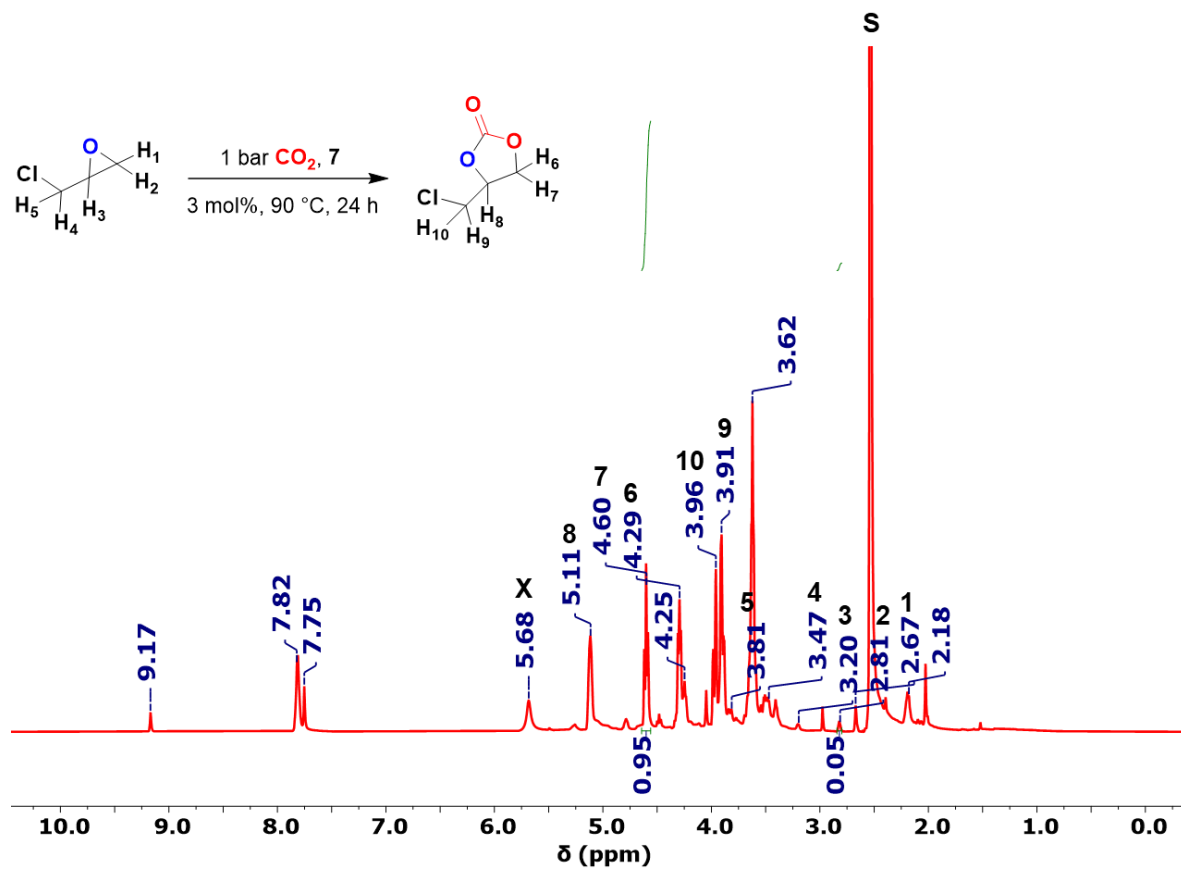


**Figure S29.** <sup>1</sup>H NMR spectrum of the conversion of ECH into its corresponding carbonate in DMSO-*d*<sub>6</sub>, **S**: solvent, **X**: 3-chloropropane-1,2-diol (from the starting material as supplied by the chemical vendor), peaks at 2.18, 3.62, 4.25, 7.75, 7.82, and 9.17 ppm correspond to the catalyst.

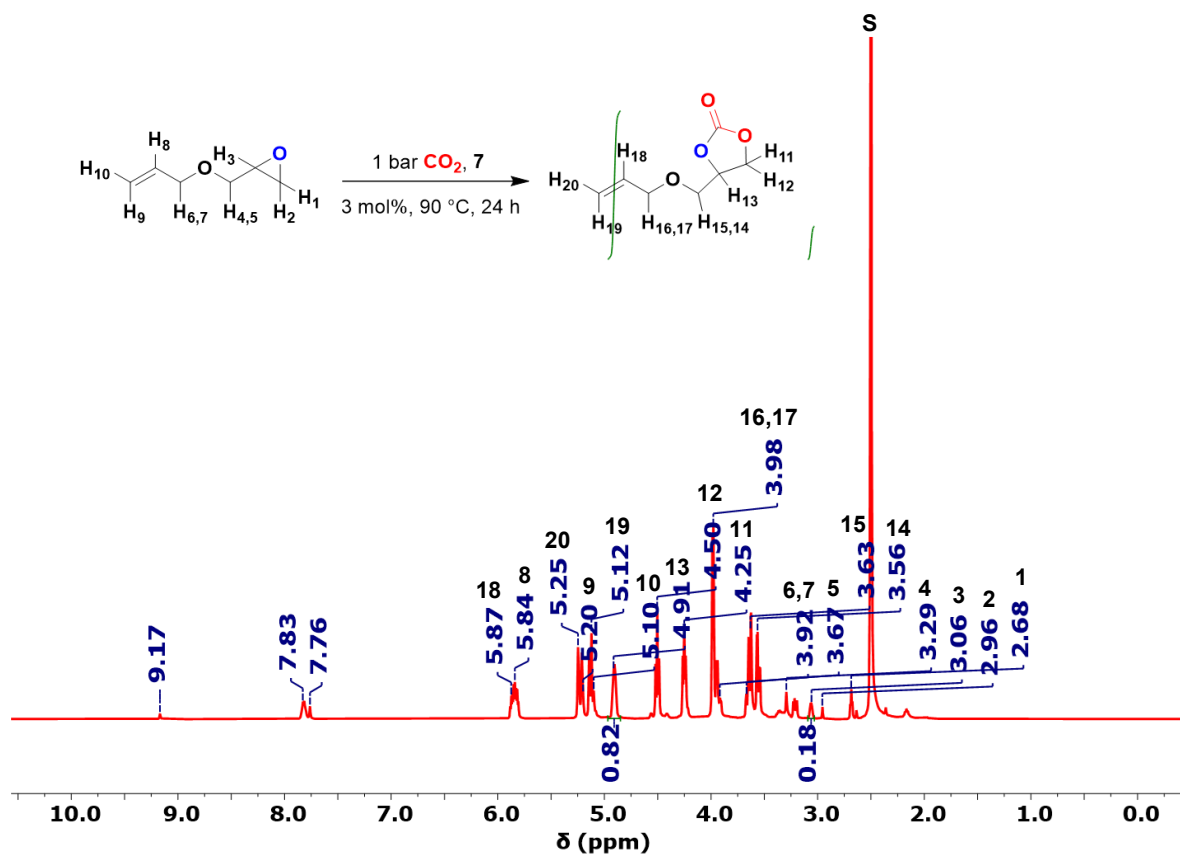


**Figure S30.**  $^1\text{H}$  NMR spectrum of the conversion of allyl glycidyl ether into its corresponding carbonate in  $\text{DMSO}-d_6$ , S: solvent. Peaks at 2.18, 3.62, 4.27, 7.76, 7.83, and 9.17 ppm correspond to the catalyst.

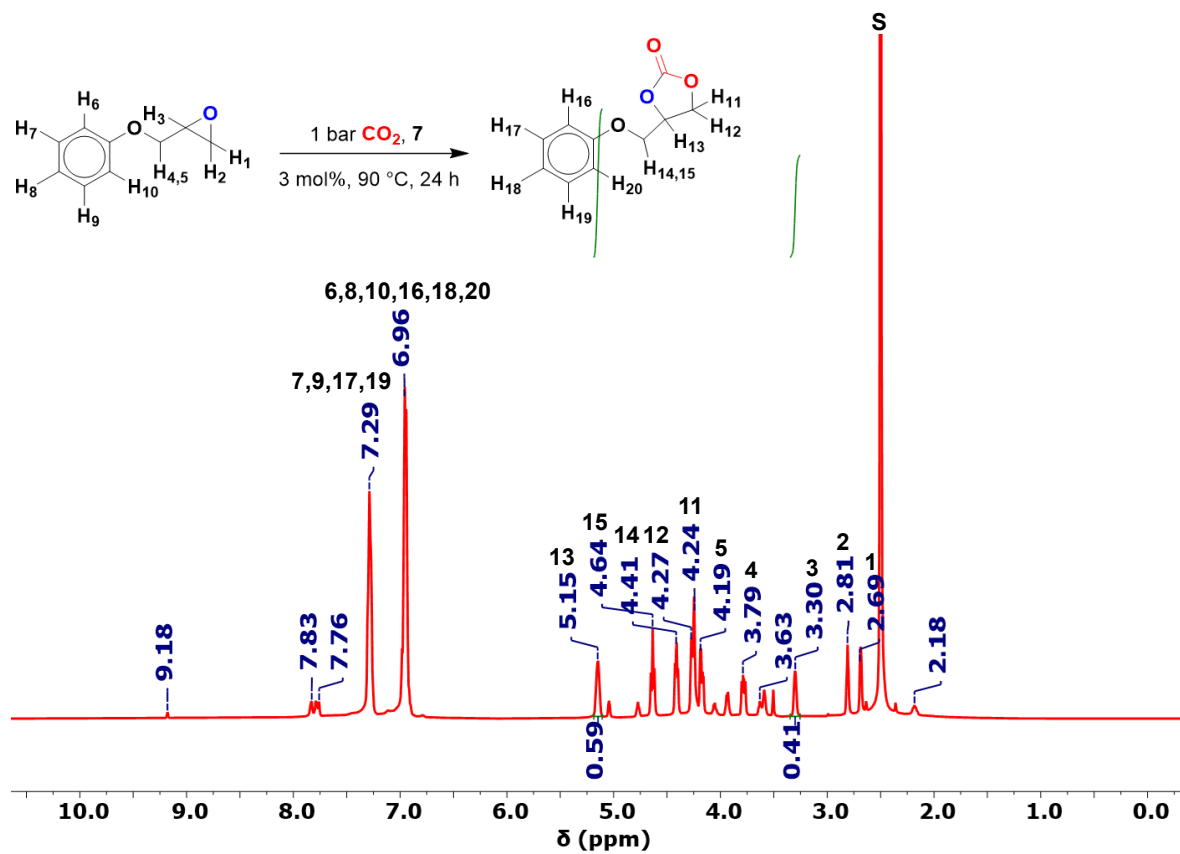


**Figure S31.**  $^1\text{H}$  NMR spectrum of the conversion of 1,2-epoxy-3-phenoxy propane into its corresponding carbonate in DMSO- $d_6$ , S: solvent. Peaks at 2.18, 3.63, 4.23, 7.76, 7.83, and 9.18 ppm correspond to the catalyst.

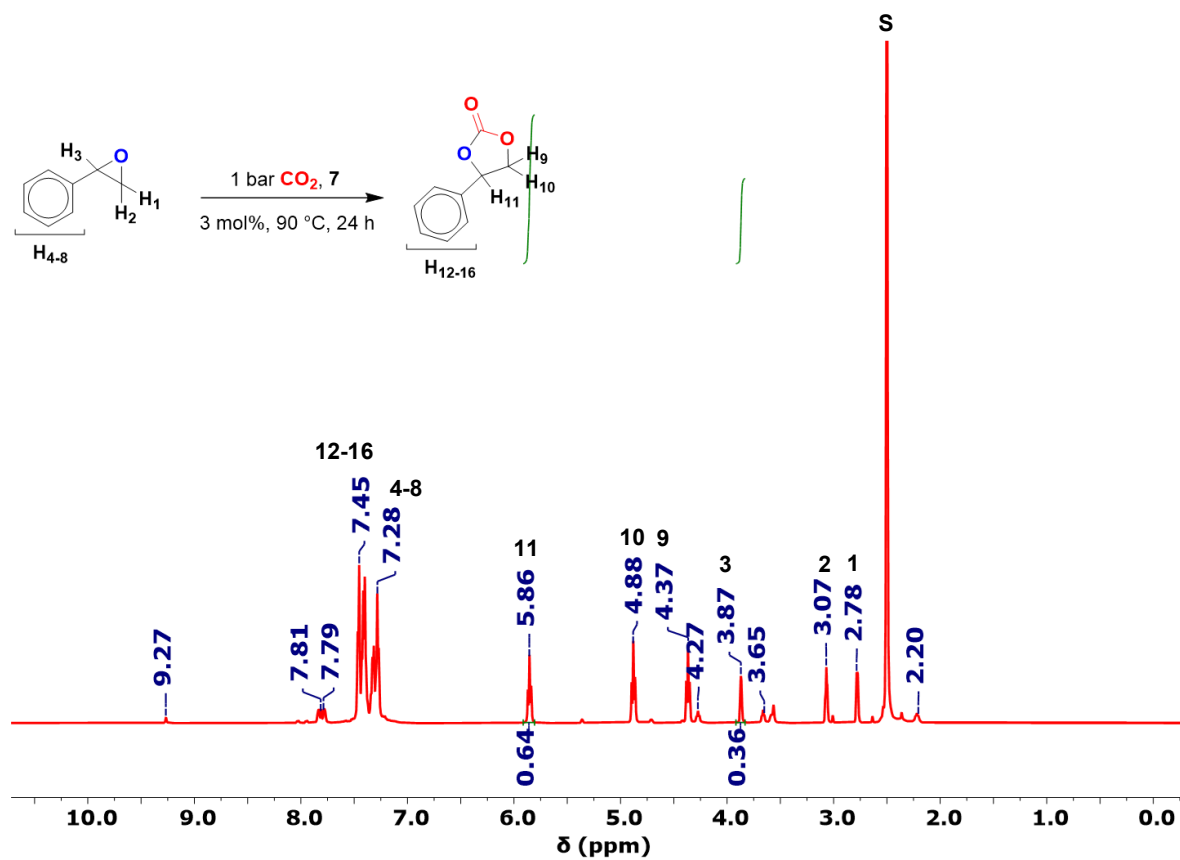


**Figure S32.** <sup>1</sup>H NMR spectrum of the conversion of styrene oxide into its corresponding carbonate in DMSO-*d*<sub>6</sub>, S: solvent. Peaks at 2.20, 3.65, 4.27, 7.79, 7.81, and 9.27 ppm correspond to the catalyst.



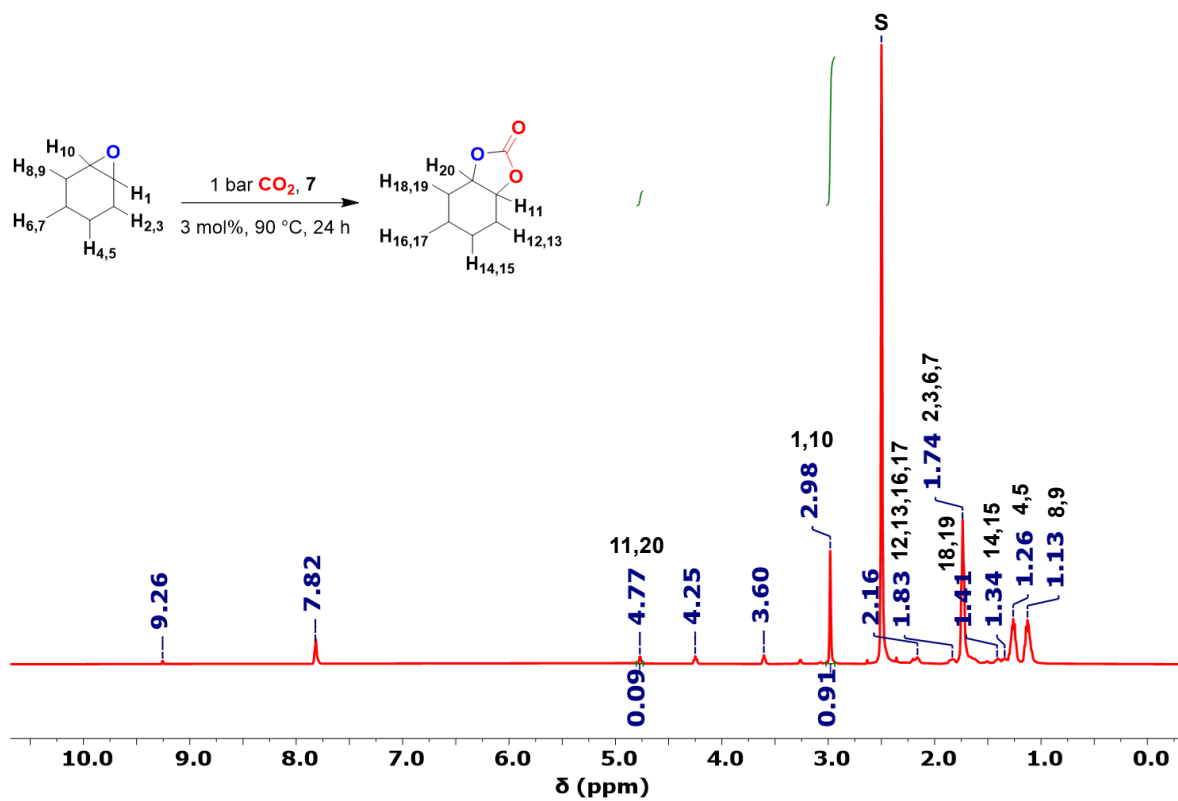


**Figure S33.** <sup>1</sup>H NMR spectrum of the conversion of cyclohexene oxide into its corresponding carbonate in DMSO-*d*<sub>6</sub>, S: solvent. Peaks at 2.16, 3.60, 4.25, 7.82, and 9.26 ppm correspond to the catalyst.

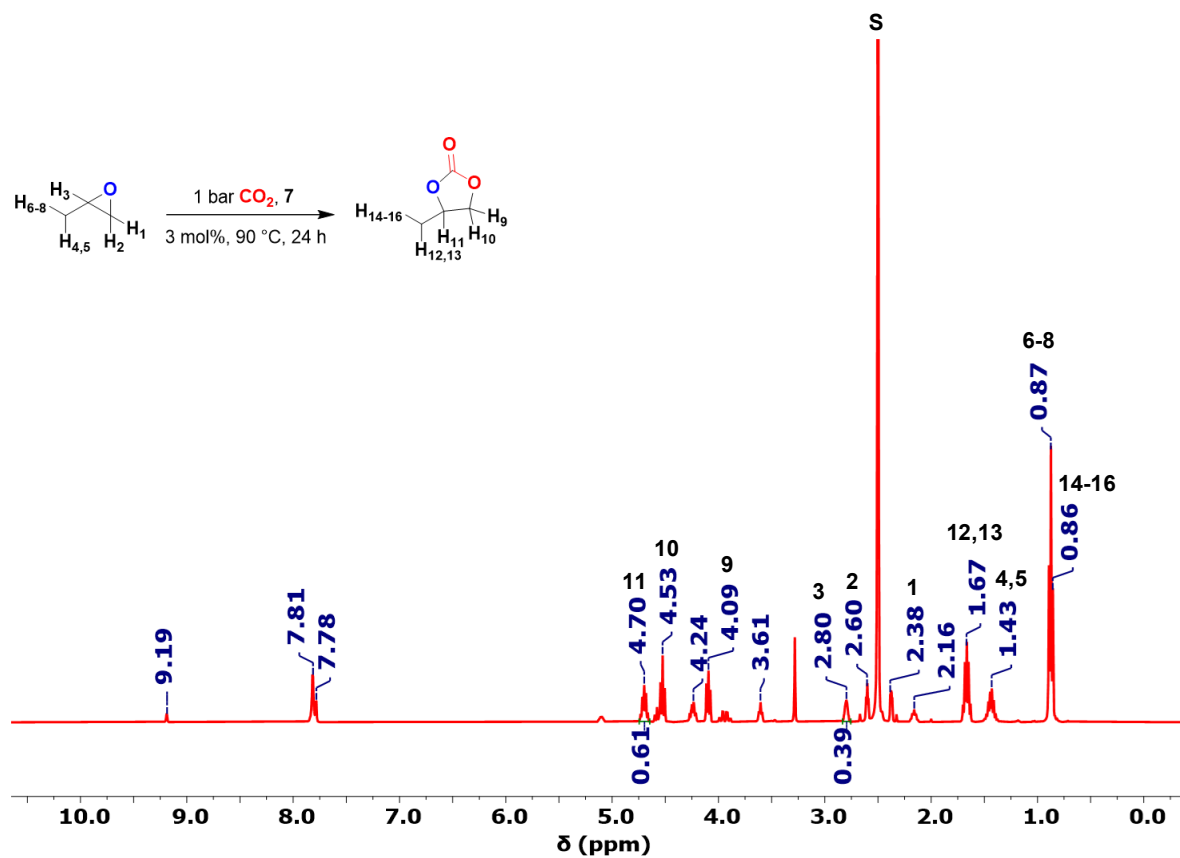


**Figure S34.**  $^1\text{H}$  NMR spectrum of the conversion of 1,2-epoxybutane into its corresponding carbonate in DMSO- $d_6$ , S: solvent. Peaks at 2.16, 3.61, 4.24, 7.78, 7.81, and 9.19 ppm correspond to the catalyst.

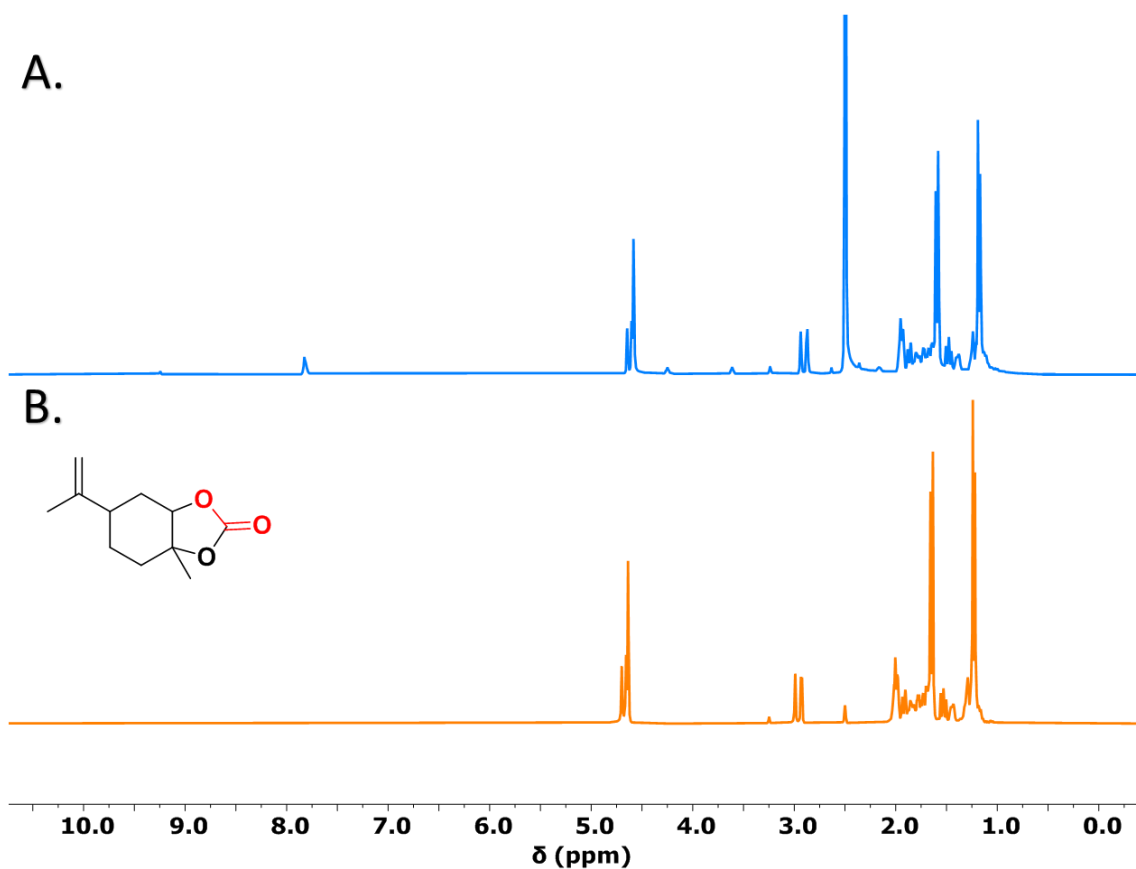


**Figure S35.**  $^1\text{H}$  NMR spectra in  $\text{DMSO}-d_6$  of: **A.** Limonene oxide coupled with  $\text{CO}_2$  in the presence of **7**, peaks at 2.17, 3.61, 4.25, 7.84 and 9.22 ppm correspond to the catalyst (blue trace); **B.** limonene oxide (orange trace). The CC peaks are not observed. Peaks at 2.18, 3.62, 4.25, 7.75, 7.82, and 9.17 ppm correspond to the catalyst.

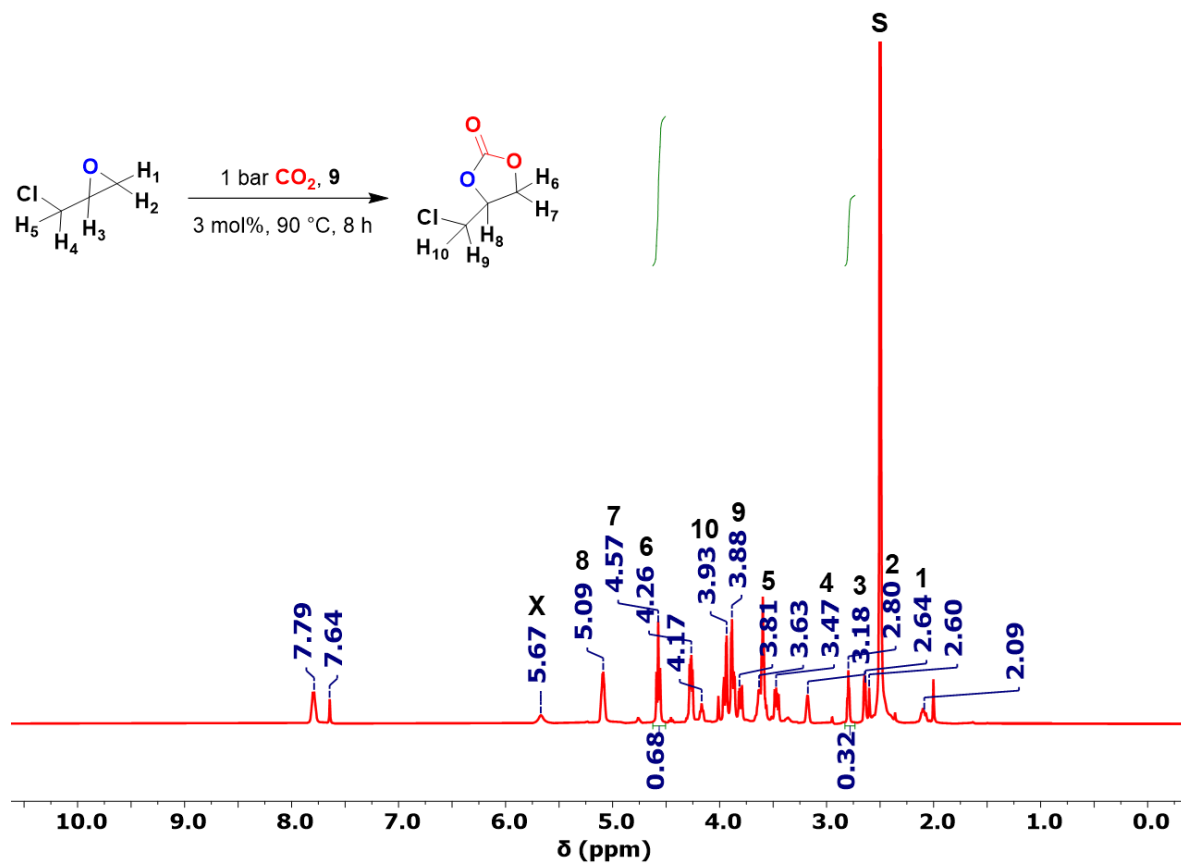


**Figure S36.**  $^1\text{H}$  NMR spectrum of the conversion of ECH into its corresponding carbonate in DMSO- $d_6$ , S: solvent, X: 3-chloropropane-1,2-diol (from the starting material purchased from the chemical vendor). Peaks at 2.09, 2.60, 3.63, 4.17, 7.64, and 7.79 ppm correspond to the catalyst.

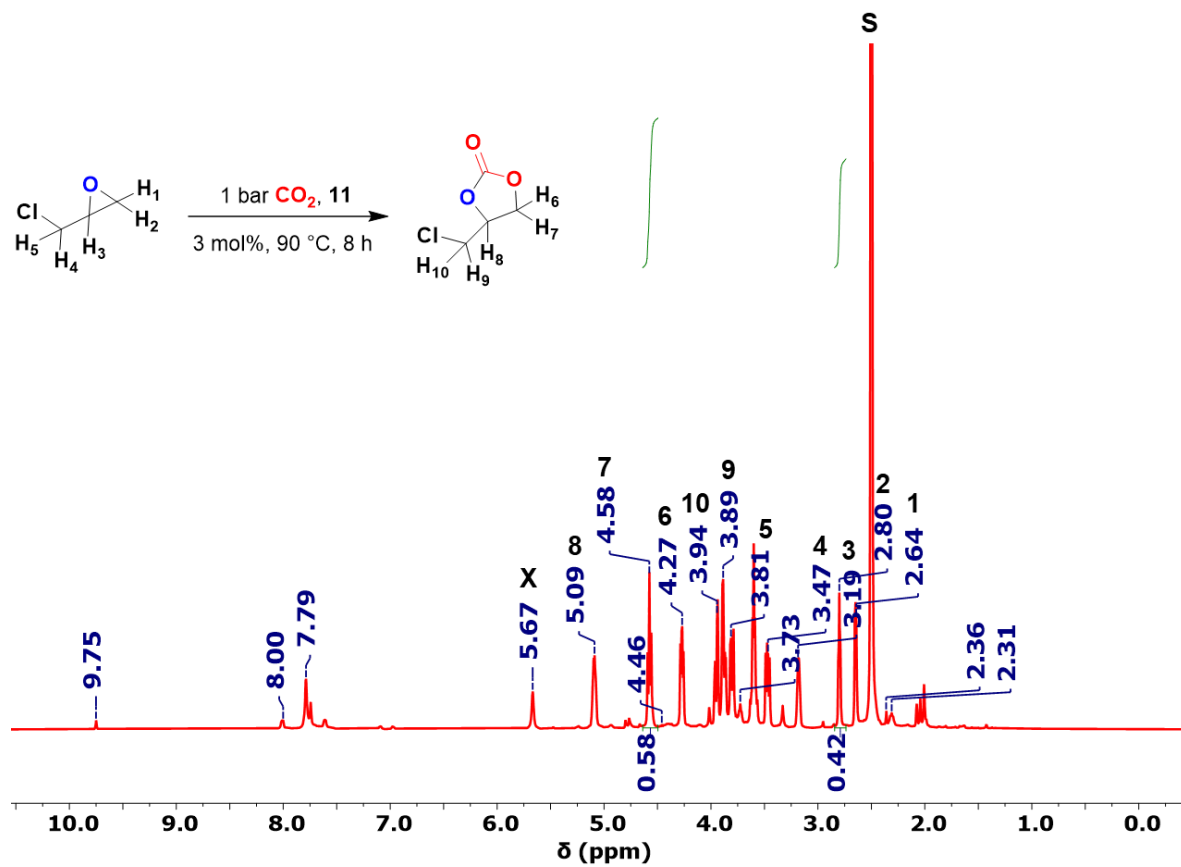


**Figure S37.** <sup>1</sup>H NMR spectrum of the conversion of ECH into its corresponding carbonate in DMSO-*d*<sub>6</sub>, **S**: solvent, **X**: 3-chloropropane-1,2-diol (from the starting material as supplied by the chemical vendor). Peaks at 2.31, 3.36, 3.73, 4.46, 7.79, 8.00, and 9.75 ppm correspond to the catalyst.

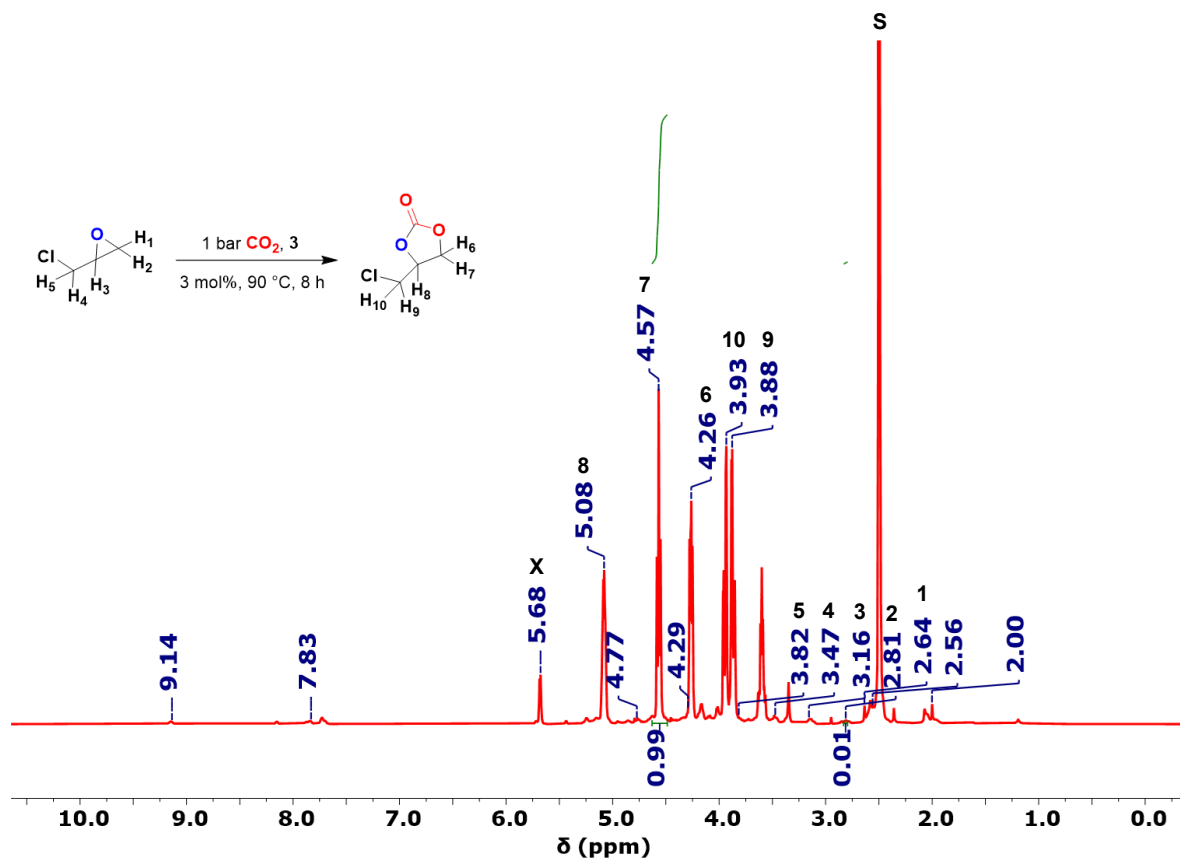


**Figure S38.**  $^1\text{H}$  NMR spectrum of the conversion of ECH into its corresponding carbonate in DMSO- $d_6$ , **S**: solvent, **X**: 3-chloropropane-1,2-diol (from the starting material as supplied by the chemical vendor). Peaks at 2.00, 2.56, 4.29, 4.77, 7.83 and 9.14 ppm correspond to the catalyst.

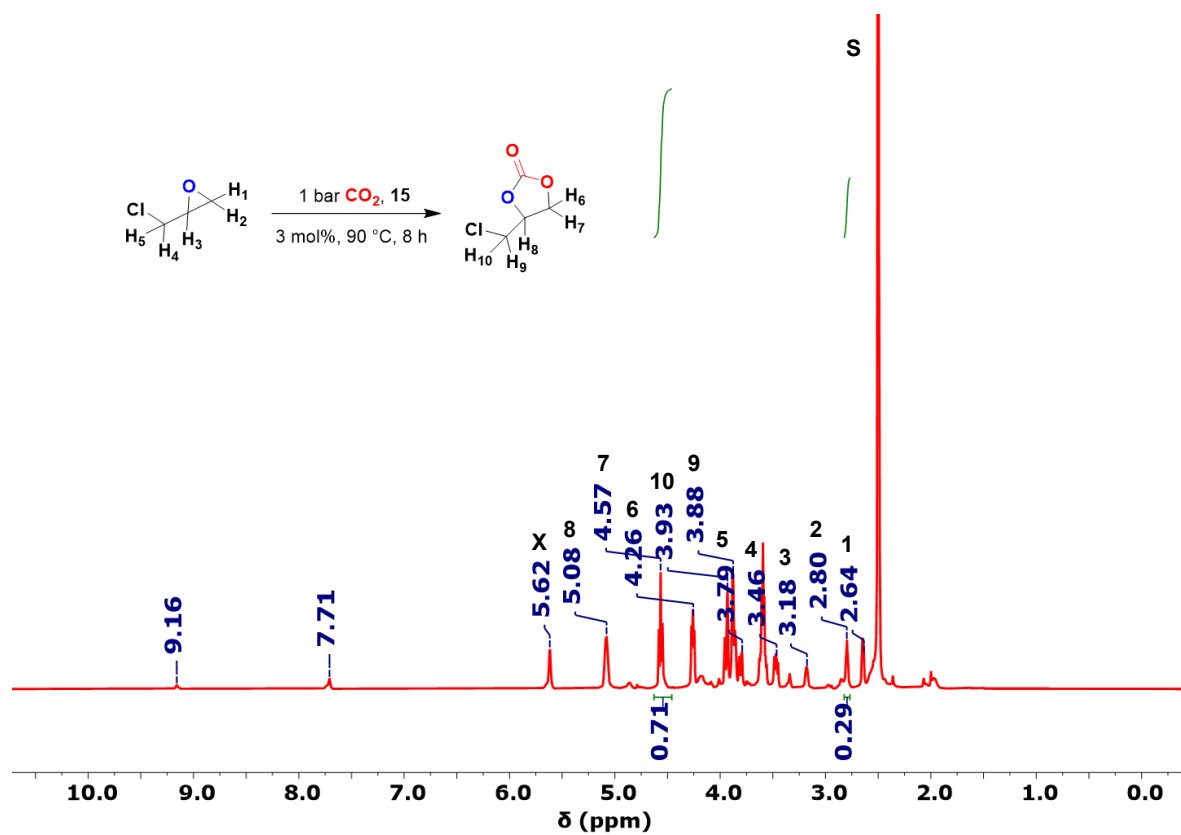


**Figure S39.**  $^1\text{H}$  NMR spectrum of the conversion of ECH into its corresponding carbonate in DMSO- $d_6$ , **S**: solvent, **X**: 3-chloropropane-1,2-diol (from the starting material as supplied by the chemical vendor). Peaks at 2.15, 2.83, 4.34, 7.71 and 9.16 ppm correspond to the catalyst.

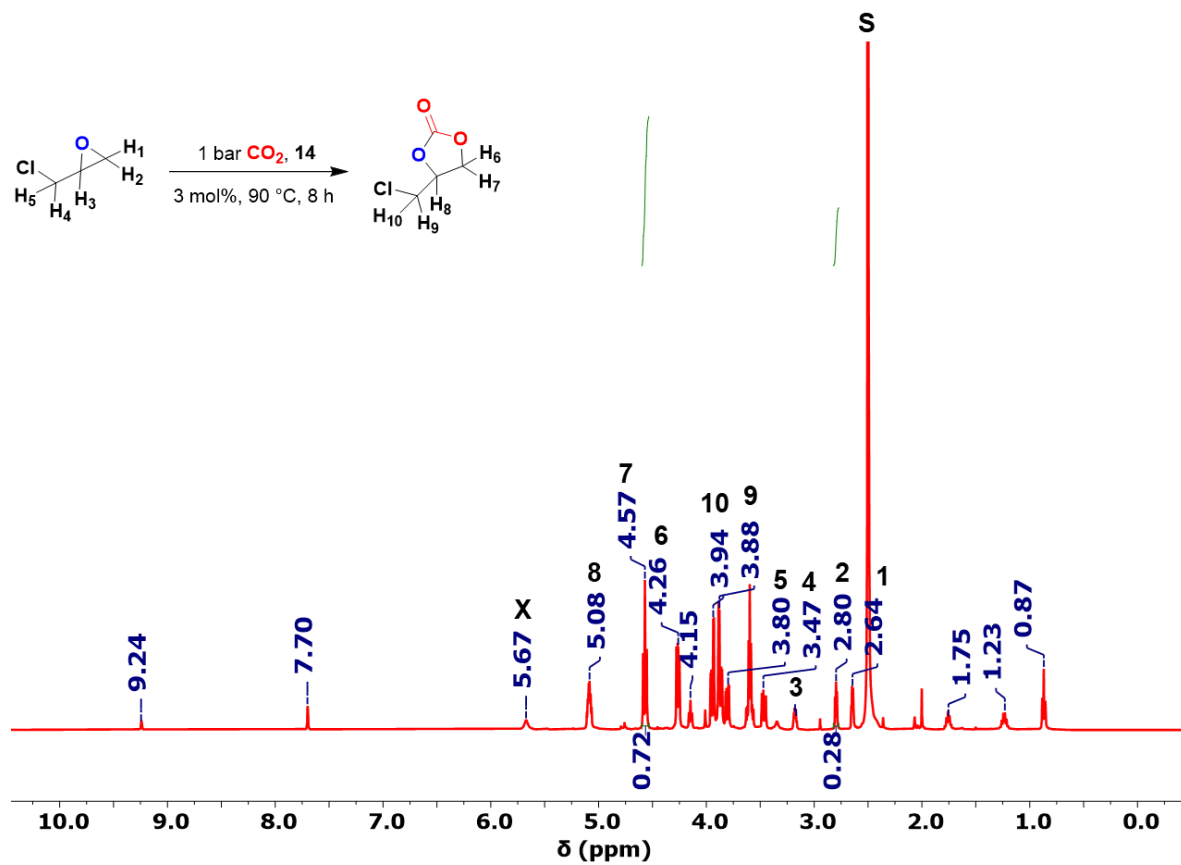


**Figure S40.** <sup>1</sup>H NMR spectrum of the conversion of ECH into its corresponding carbonate in DMSO-*d*<sub>6</sub>, S: solvent, X: 3-chloropropane-1,2-diol (from the starting material as supplied by the chemical vendor). Peaks at 0.87, 1.23, 1.75, 4.15, 7.70 and 9.24 ppm correspond to the catalyst.



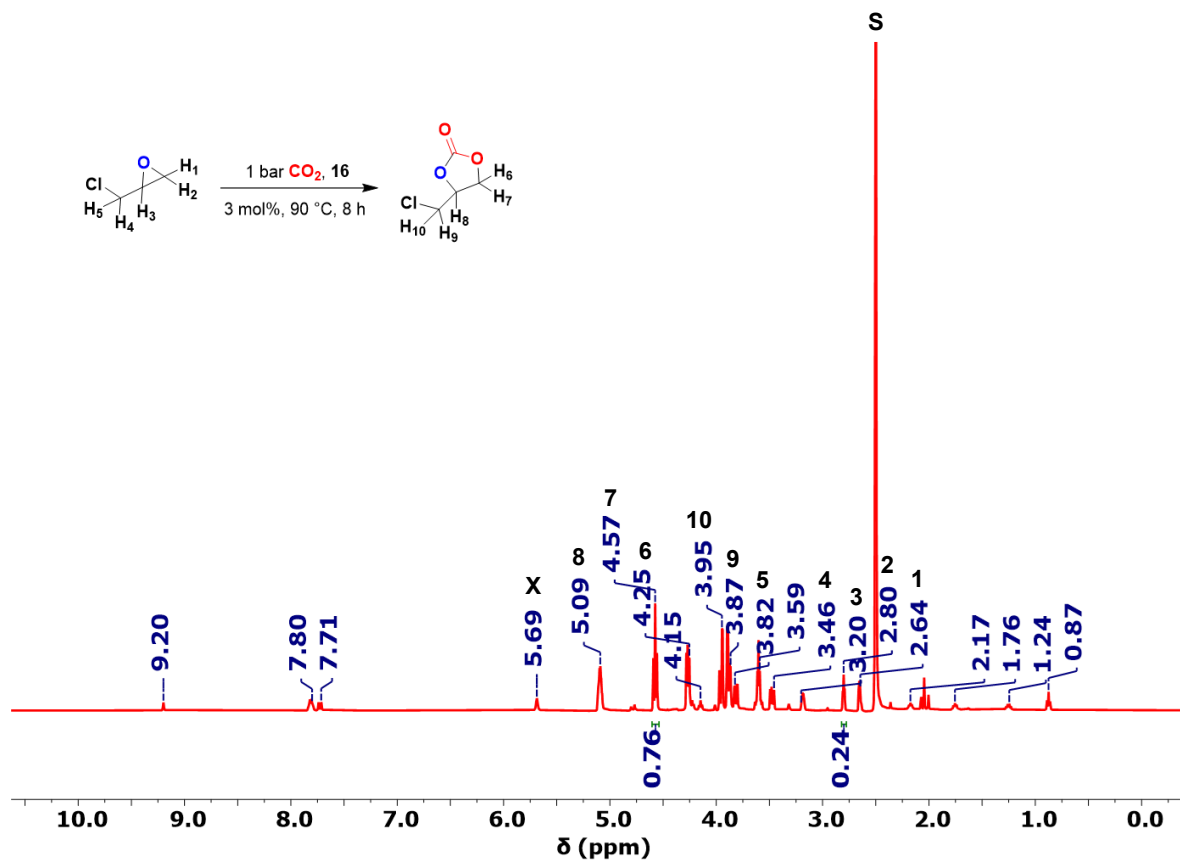


**Figure S41.** <sup>1</sup>H NMR spectrum of the conversion of ECH into its corresponding carbonate in DMSO-*d*<sub>6</sub>, **S**: solvent, **X**: 3-chloropropane-1,2-diol (from the starting material as supplied by the chemical vendor). Peaks at 0.87, 1.24, 1.76, 2.17, 3.59, 4.15, 7.71, 7.80 and 9.20 ppm correspond to the catalyst.

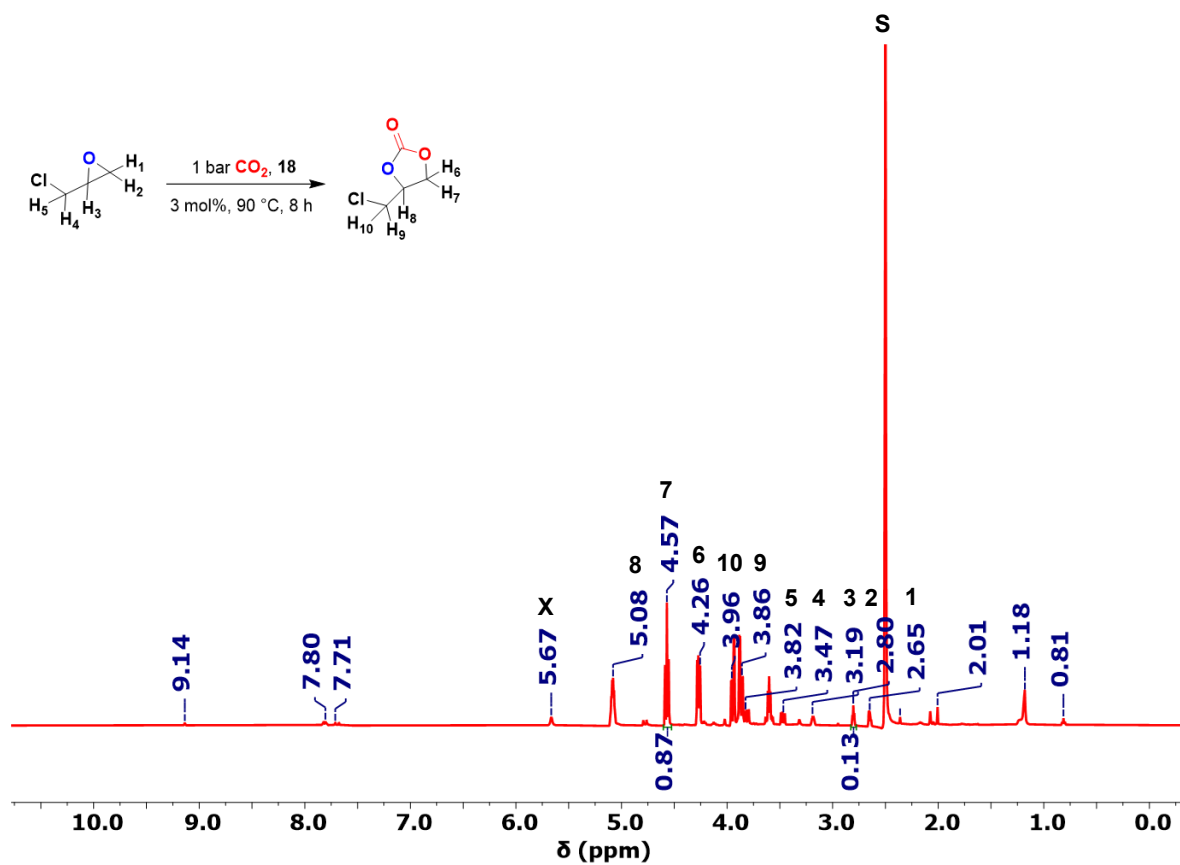


**Figure S42.**  $^1\text{H}$  NMR spectrum of the conversion of ECH into its corresponding carbonate in  $\text{DMSO}-d_6$ , **S**: solvent, **X**: 3-chloropropane-1,2-diol (from the starting material as supplied by the chemical vendor). Peaks at 0.81, 1.18, 2.01, 3.73, 4.34, 4.46, 7.71, 7.80 and 9.14 ppm correspond to the catalyst.

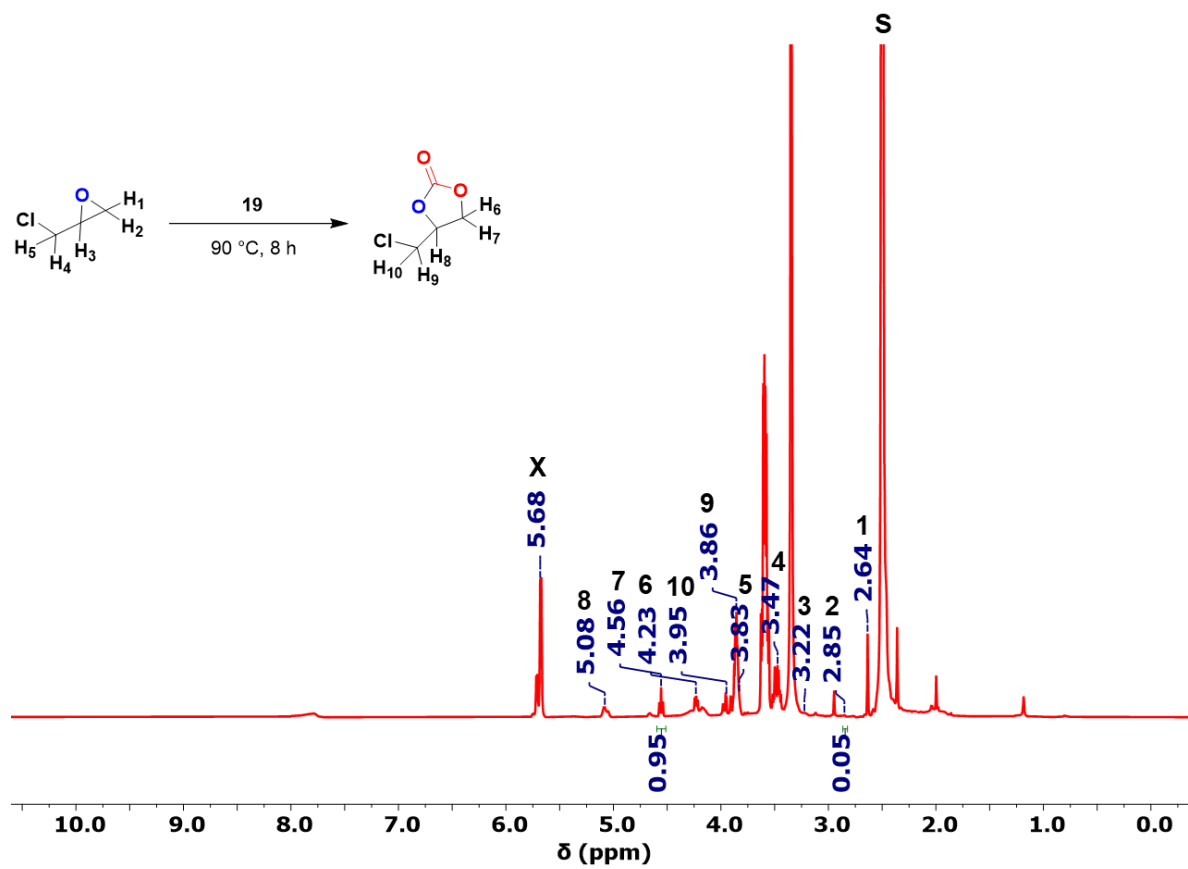


**Figure S43.** <sup>1</sup>H NMR spectrum of the conversion of ECH into its corresponding carbonate in DMSO-*d*<sub>6</sub>, S: solvent, X: 3-chloropropane-1,2-diol (from the starting material as supplied by the chemical vendor).

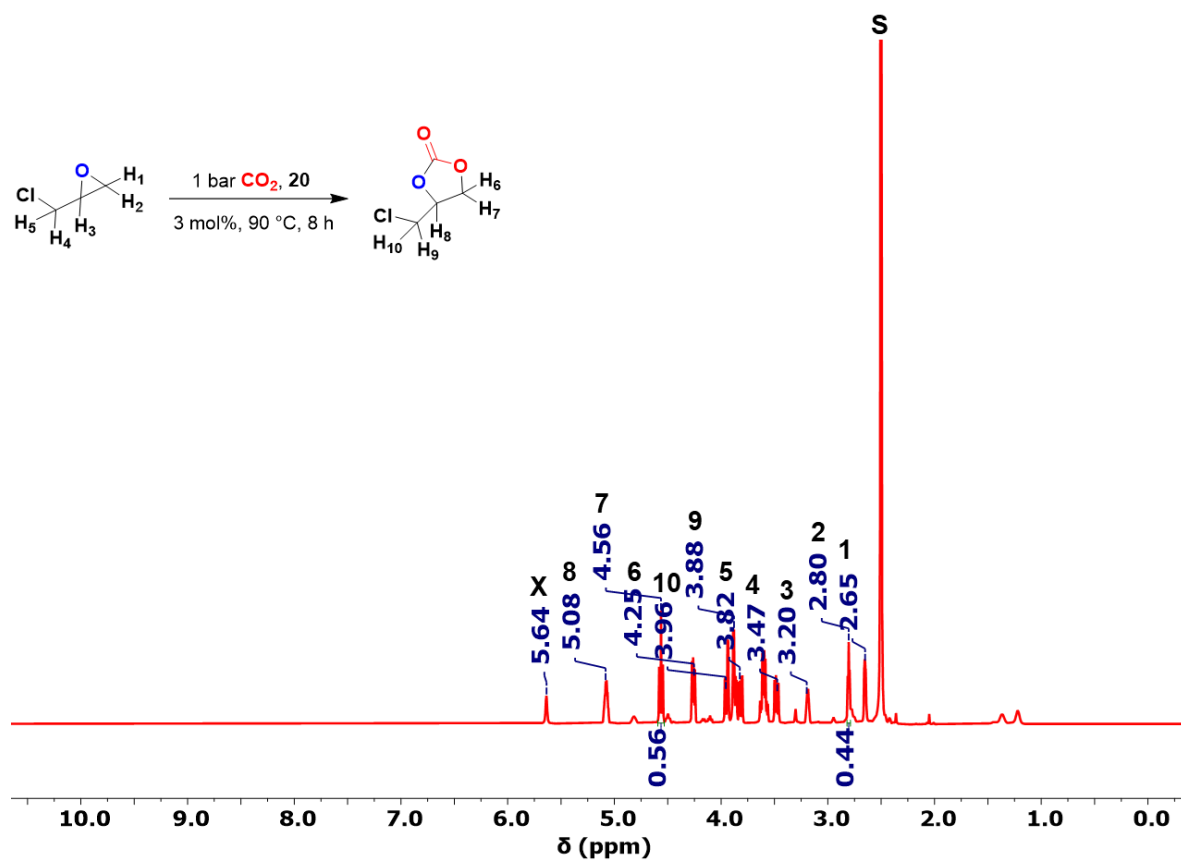


**Figure S44.** <sup>1</sup>H NMR spectrum of the conversion of ECH into its corresponding carbonate in DMSO-*d*<sub>6</sub>, S: solvent, X: 3-chloropropane-1,2-diol (from the starting material as supplied by the chemical vendor).

### 3.3 <sup>1</sup>H NMR spectra for CCs Isolation

For CC isolation, the catalyst was removed from the reaction mixture by adding 20 mL of EtOAc for all cycloaddition reactions, except when dealing with ECH crude mixture, 40 mL was added. The catalyst was filtered out, washed with 40 mL EtOAc, then the filtrate was concentrated. The desired CC was isolated through a *silica plug* and monitored *via* thin layer chromatography. SO/Styrene carbonate (4-phenyl-1,3-dioxolan-2-one) crude mixture was eluted with a 1:1 (v/v) ratio of hexane/EtOAc, the collected fractions were concentrated using a rotary evaporator. Once cooled at RT, a liquid concentrate was obtained, in which *ca.* 10 mL hexane/EtOAc was used to dissolve the concentrate, where crystallization was induced upon slight heating, left to cool at RT, then stored in a freezer at -20°C for 2d, which resulted in the formation of a white crystalline solid, which was filtered, dried, and identified spectroscopically accordingly. The same procedure was applied with 4-(phenoxyethyl)-1,3-dioxolan-2-one. While (2:1) and (3:1) ratio (by volume) were used for the elution of 4-chloromethyl-2-oxo-1,3-dioxolane together with 4-ethyl-1,3-dioxolan-2-one crude mixtures, respectively. For 4-((allyloxy)methyl)-1,3-dioxolan-2-one, neat hexane was passed over the *plug* to isolate its unreacted epoxide, then EtOAc was used to isolate CC. Liquid carbonates were isolated and dried at 60 °C under vacuum.

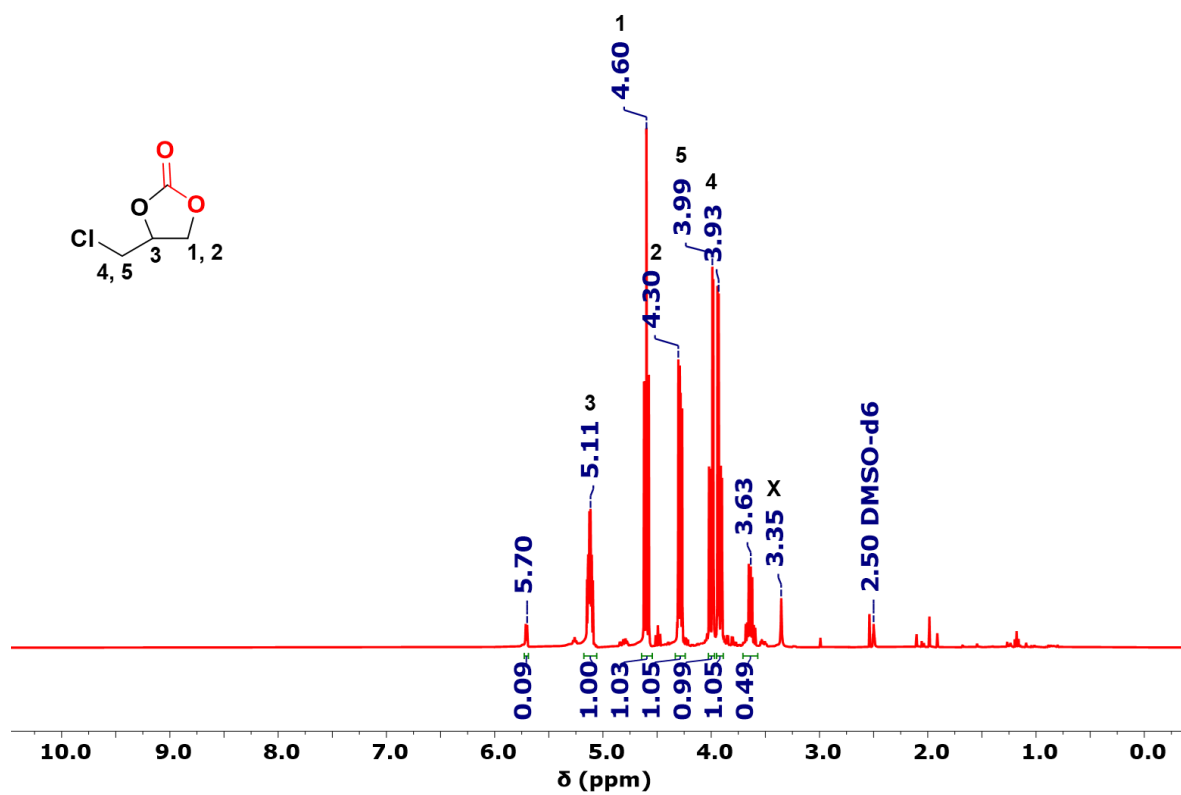


**Figure S45.** <sup>1</sup>H NMR spectrum of the isolated 4-chloromethyl-2-oxo-1,3-dioxolane in DMSO-*d*<sub>6</sub>, X: water, traces peaks at 5.70, and 3.63 correspond to 3-chloropropane-1,2-diol.

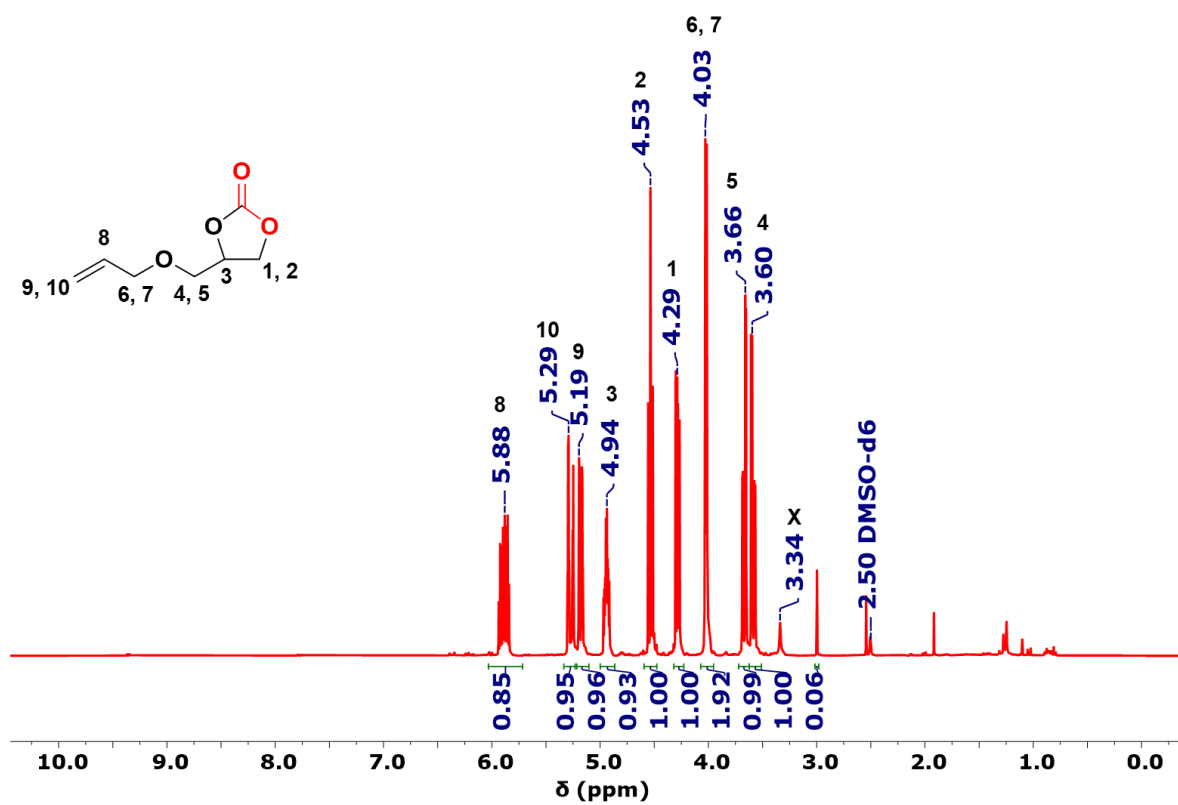


**Figure S46.**  $^1\text{H}$  NMR spectrum of the isolated 4-((allyloxy)methyl)-1,3-dioxolan-2-one in  $\text{DMSO-}d_6$ , X: water.

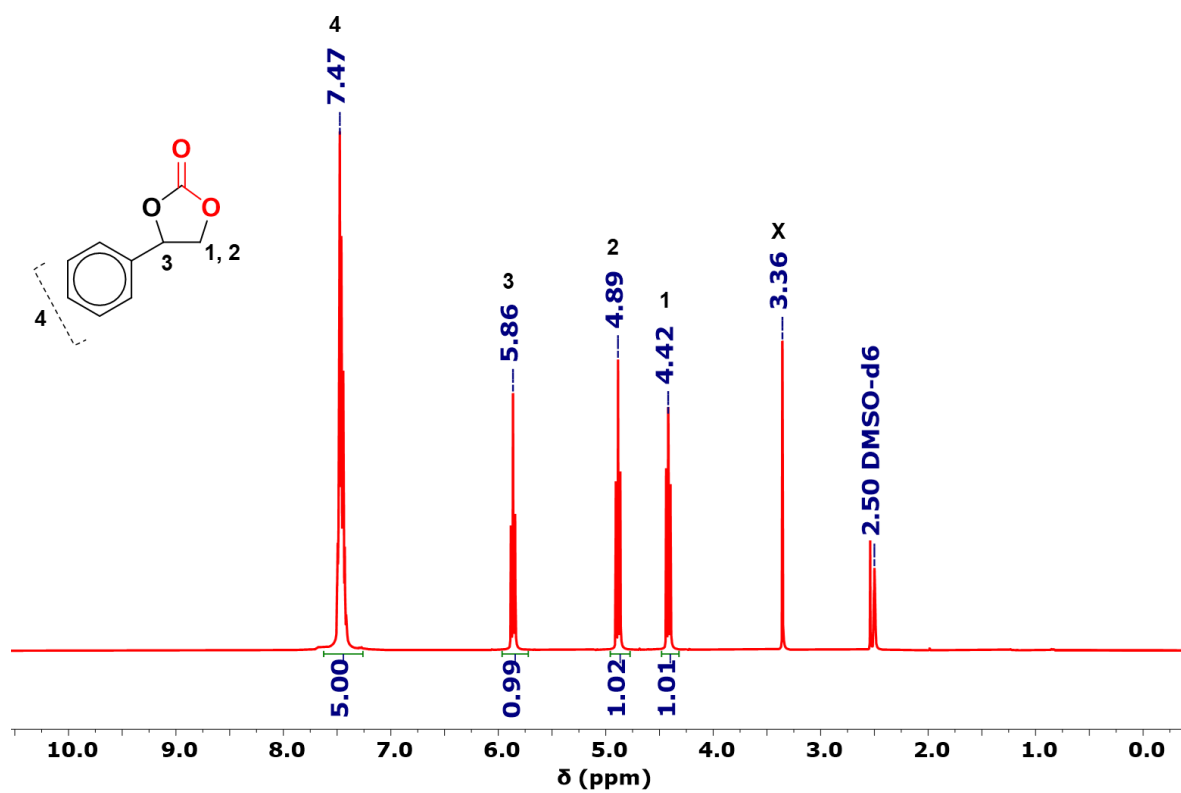


**Figure S47.** <sup>1</sup>H NMR spectrum of the isolated 4-phenyl-1,3-dioxolan-2-one in DMSO-*d*<sub>6</sub>, X: water.



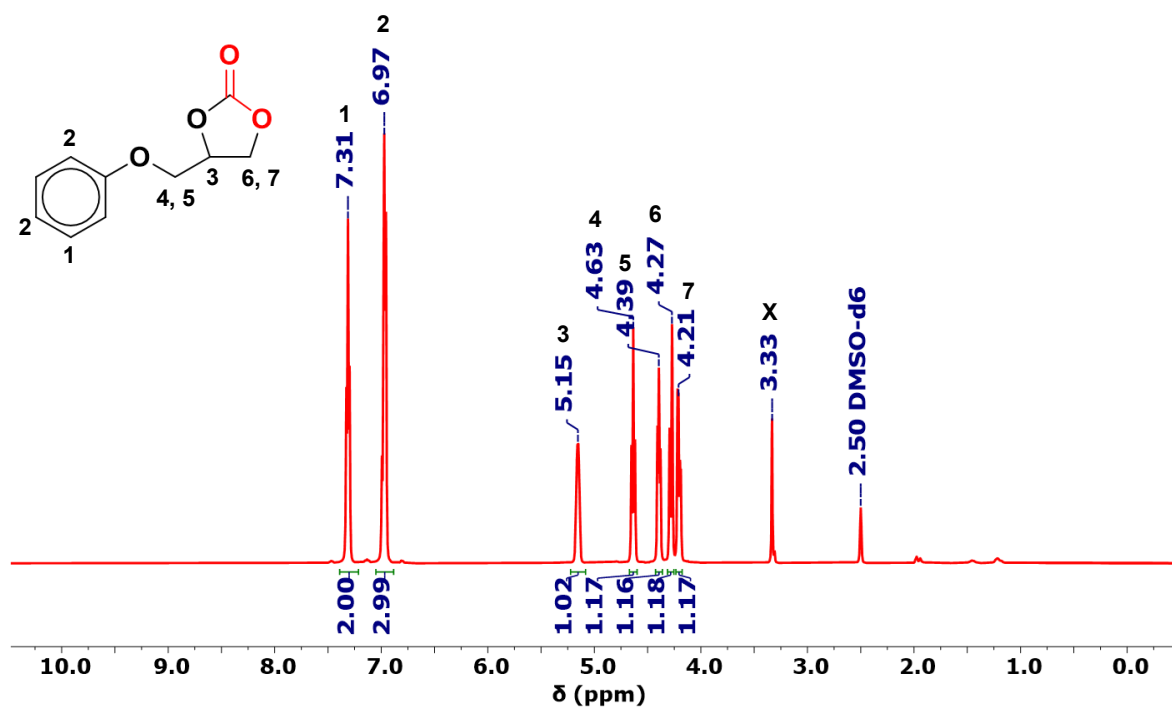


**Figure S48.**  $^1\text{H}$  NMR spectrum of 4-(phenoxymethyl)-1,3-dioxolan-2-one in  $\text{DMSO-}d_6$ , X: water.

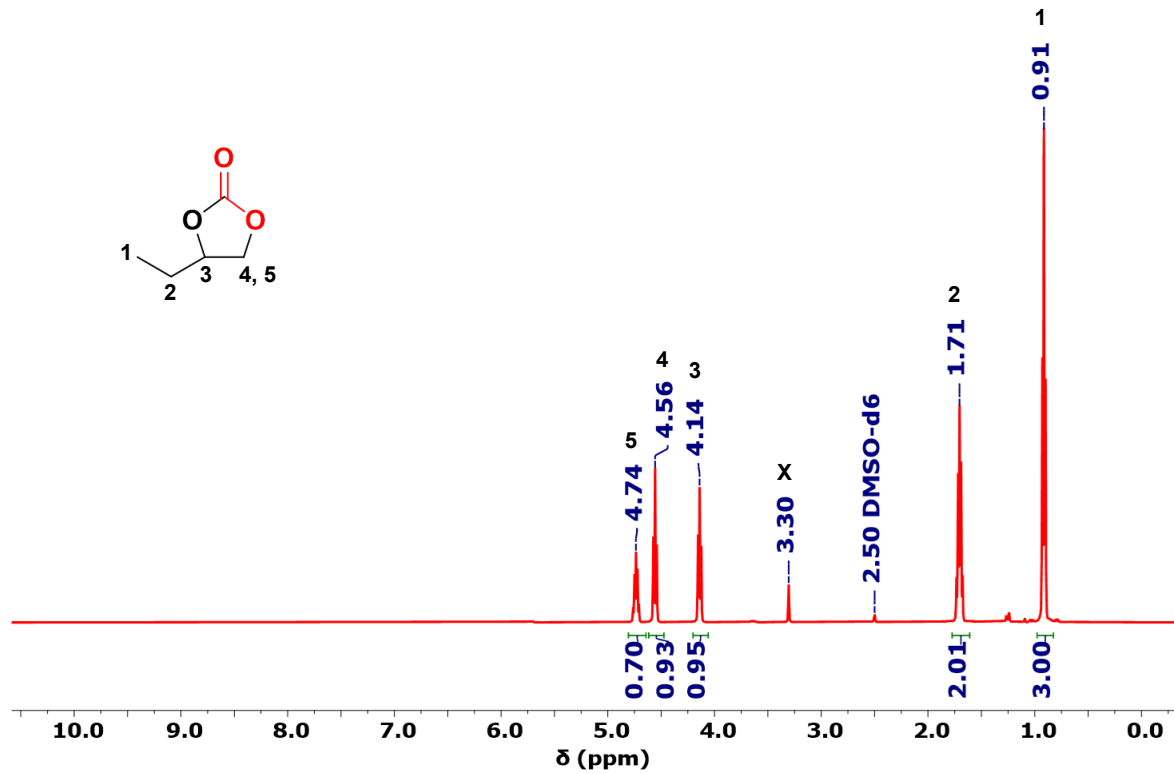


**Figure S49.**  $^1\text{H}$  NMR spectrum of 4-ethyl-1,3-dioxolan-2-one in DMSO- $d_6$ , X: water.

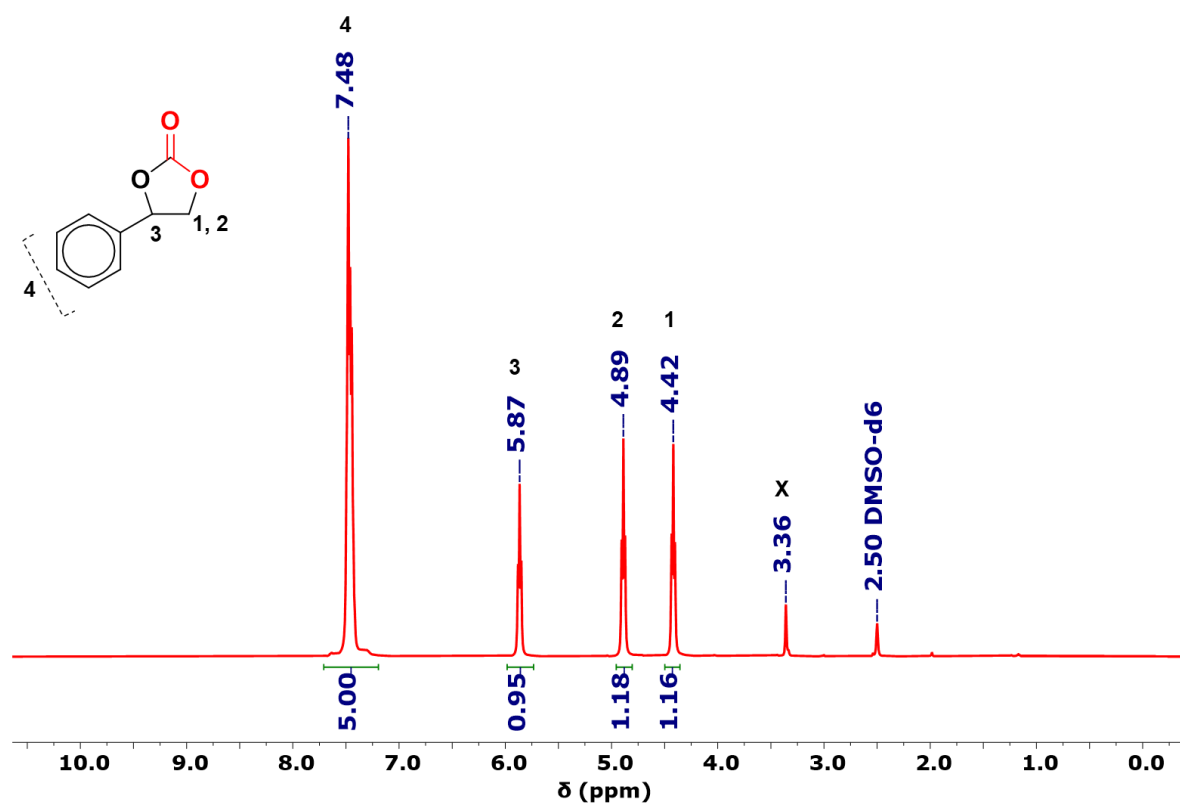
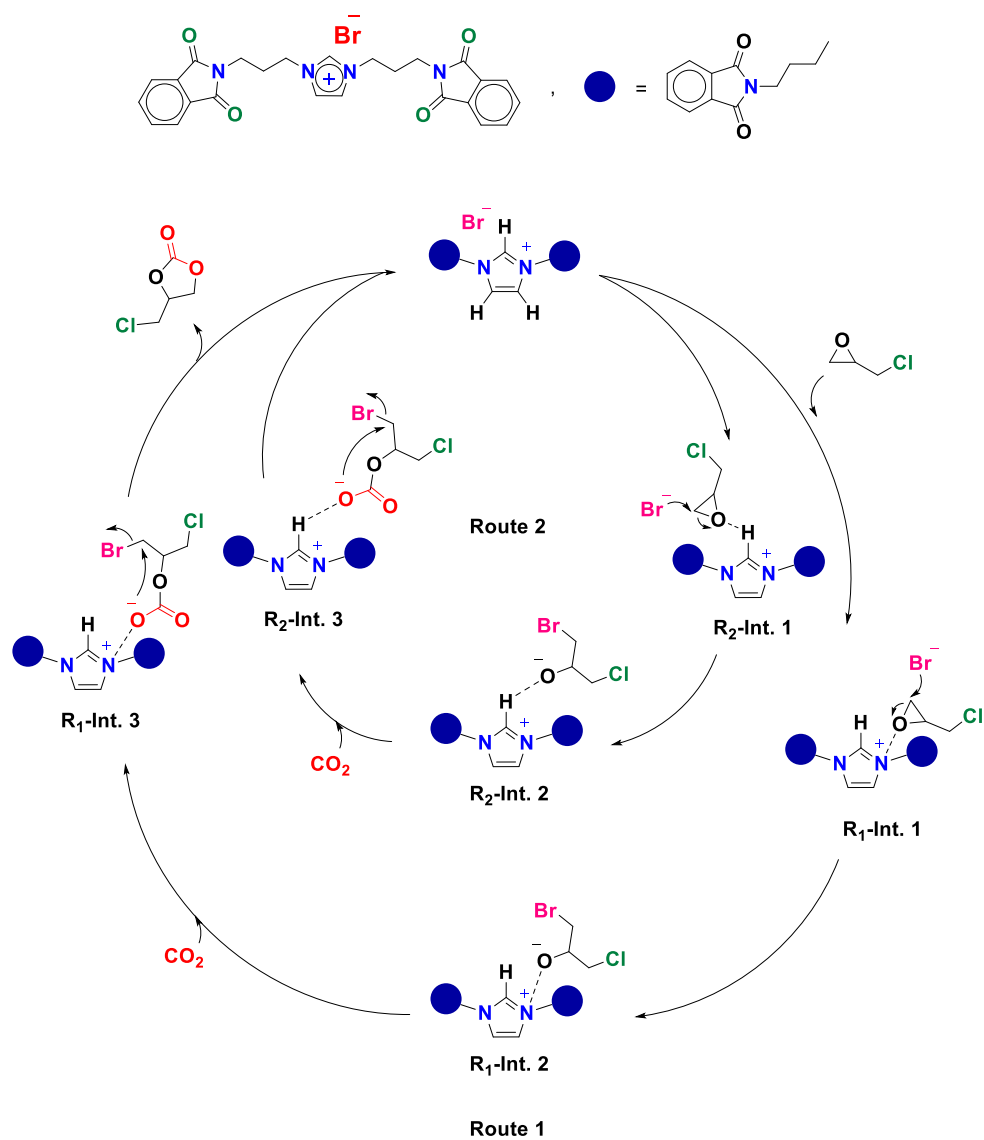
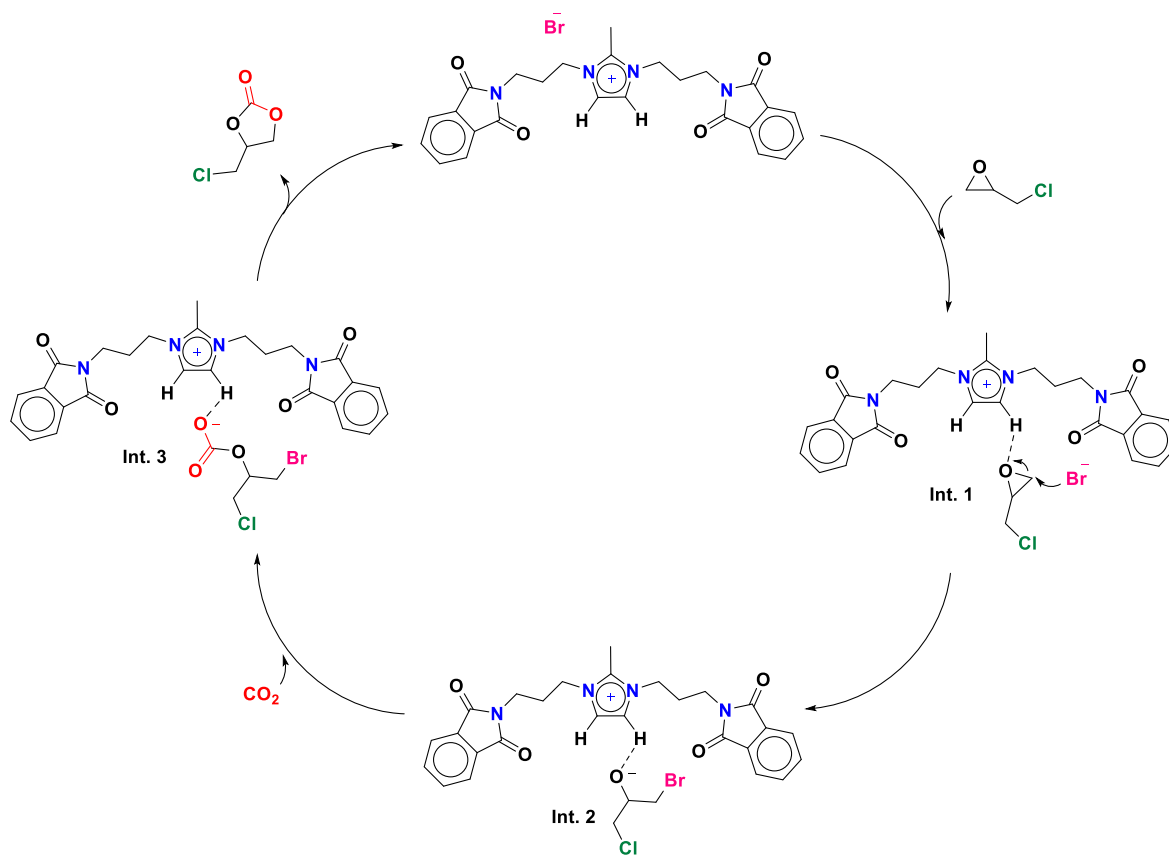


**Figure S50.** <sup>1</sup>H NMR spectrum of 4-phenyl-1,3-dioxolan-2-one in DMSO-*d*<sub>6</sub> isolated from the recyclability run, **X**: water.

## 4 Proposed mechanisms of the cycloaddition reaction



**Scheme S9.** Proposed reaction mechanism of ECH conversion into its corresponding carbonate using catalyst 7.



**Scheme S10.** Proposed reaction mechanism of ECH conversion into its corresponding carbonate using catalyst **9**.

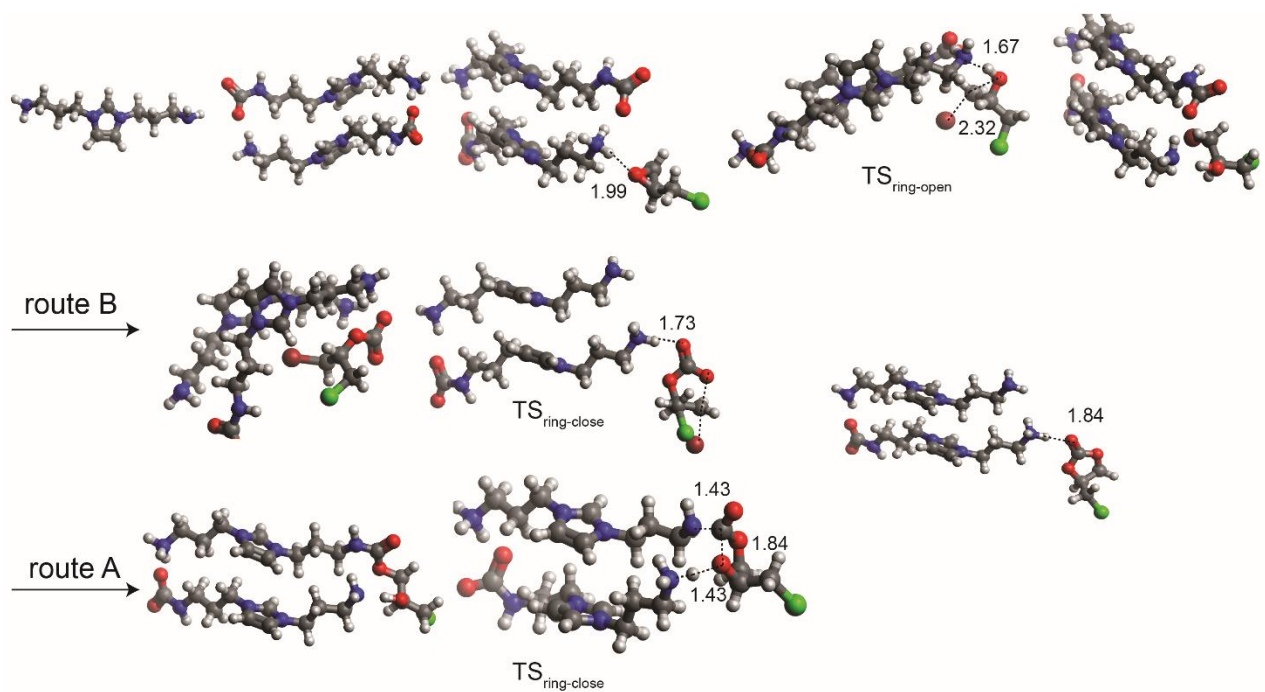


**Figure S51.** DFT-optimized molecular geometries of the species present in the reaction profile of ECH and CO<sub>2</sub>, see Figure 9A.

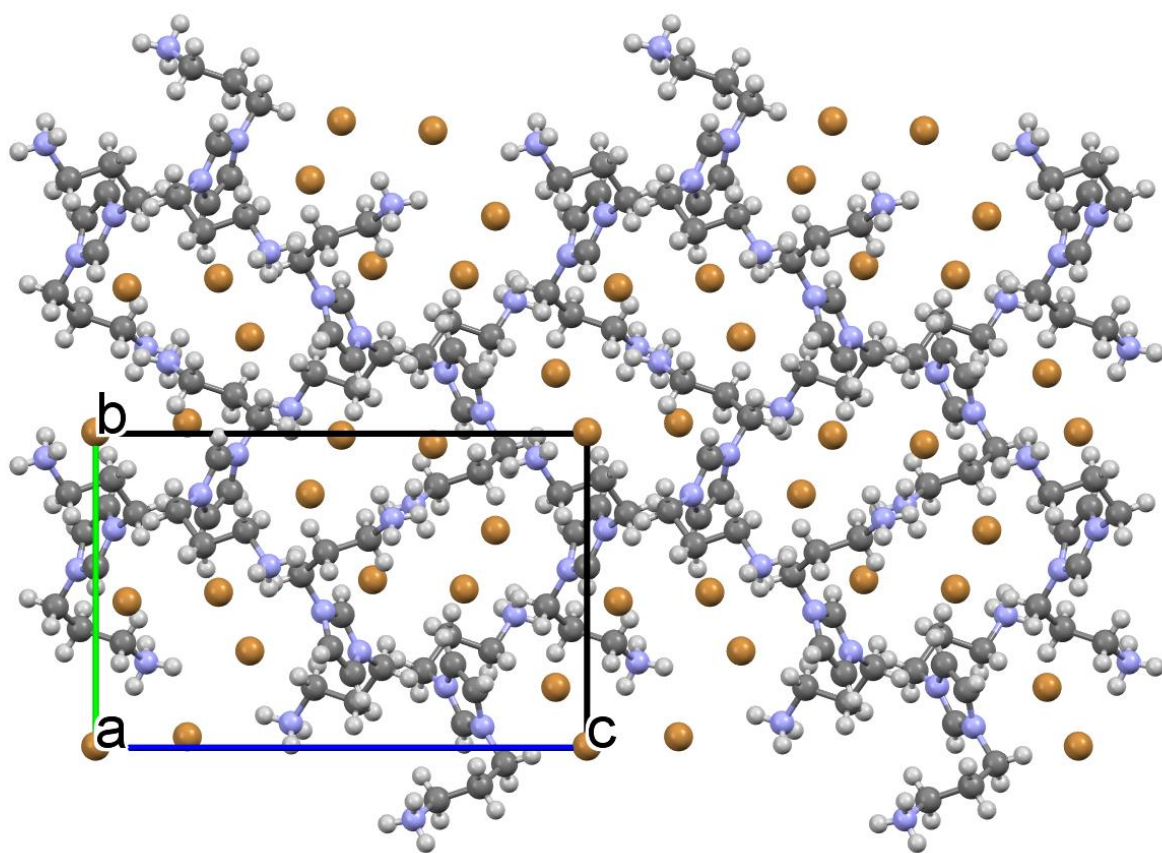


**Figure S52.** Packing diagram of **15** viewed down the a-axis.

**Table S1.** Crystal data and structure refinement for **15**

Empirical formula	C <sub>9</sub> H <sub>21</sub> N <sub>4</sub> Br <sub>3</sub>
Formula weight	425.03
Temperature/K	293(2)
Crystal system	tetragonal
Space group	P4 <sub>3</sub> 2 <sub>1</sub> 2
a/Å	9.9901(2)
b/Å	9.9901(2)
c/Å	15.6499(4)
Volume/Å <sup>3</sup>	1561.89(7)
Z	4
$\rho_{\text{calc}}/\text{g}/\text{cm}^3$	1.807
$\mu/\text{mm}^{-1}$	7.733
F(000)	832.0
Crystal size/mm <sup>3</sup>	0.3 × 0.2 × 0.1
Radiation	Mo K $\alpha$ ( $\lambda$ = 0.71073)
2 $\Theta$ range for data collection/°	5.768 to 58.674
Index ranges	-13 ≤ h ≤ 13, -13 ≤ k ≤ 13, -21 ≤ l ≤ 12
Reflections collected	7829
Independent reflections	1887 [ $R_{\text{int}}$ = 0.0304, $R_{\text{sigma}}$ = 0.0367]
Data/restraints/parameters	1887/0/75
Goodness-of-fit on F <sup>2</sup>	1.060
Final R indexes [ $I \geq 2\sigma(I)$ ]	$R_1$ = 0.0360, $wR_2$ = 0.0514
Final R indexes [all data]	$R_1$ = 0.0551, $wR_2$ = 0.0556
Largest diff. peak/hole / e Å <sup>-3</sup>	0.58/-0.56



## 5 References

- (1) Curtin, D. Y.; Schmukler, S. The Axial Effect in the Rearrangement with Nitrous Acid of Cis- and Trans-2-Amino-1-Phenylcyclohexanol. *J. Am. Chem. Soc.* **1955**, 77 (5), 1105–1110. <https://doi.org/10.1021/ja01610a008>.
- (2) Eftaiha, A. F.; Qaroush, A. K.; Abo-shunnar, A. S.; Hammad, S. B.; Assaf, K. I.; Al-Qaisi, F. M.; Paige, M. F. Interfacial Behavior of Modified Nicotinic Acid as Conventional/Gemini Surfactants. *Langmuir* **2022**, 38 (28), 8524–8533. <https://doi.org/10.1021/acs.langmuir.2c00596>.